CHAPTER 3

EXPERIMENTAL RESULTS

The present experiment has been carried out on the North Bengal University campus (at an atmospheric depth ~ 1000 gcm^{-2}) by using the NBU air shower array comprising nineteen electron density detectors , eight fast timing detectors and two muon magnetic spectrographs. A total of 16,000 shower data associated with 2927 muon events have been collected carrying out the experiment during the period January 1994 to September 1995. Showers are detected in the size range 10^4 - $2.5x10^6$ particles . Showers having chi-square per degree of freedom greater than 6 are rejected as the fit of the observed data with fitting function is poor above 6 and for the same reason showers with age parameter greater than 1.6 or less than 0.7 are also rejected .The frequency distribution of shower size and shower age are shown in fig.3.1and fig.3.2.

The results of the experiment are presented here into two sections (section 3A and section 3B)

In the first section the results on the observations made on radial distribution of electrons , radial distribution and energy spectra of muons, variation of muon density to electron density ratio as a function of radial diastance, variation of total number of muons (N_μ) with shower size (N_e) are given .

The second section includes the results dealing with the variation of primary mass with the energy of the primary particle.

SECTION - 3A

3A.1 Determination of mean primary energy :

The primary energy of an EAS event is not possible to be determined precisely from the observed particle density distribution due to the presence of fluctuations in an EAS development . However the mean primary energy was determined by comparing the observed vertical shower size with the results of Monte Carlo model for proton primary at sea-level.

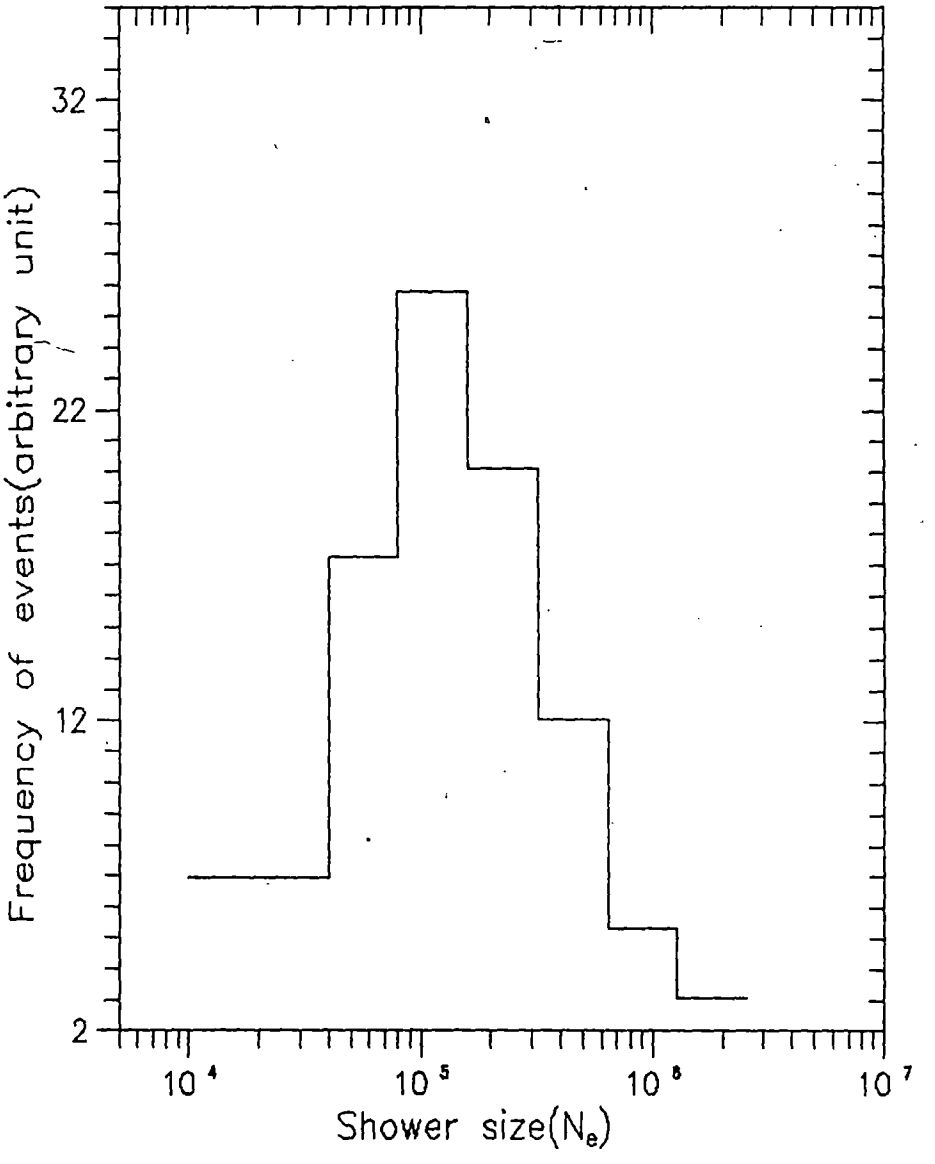

Fig.3.1. Frequency distribution of shower size of the observed shower events.

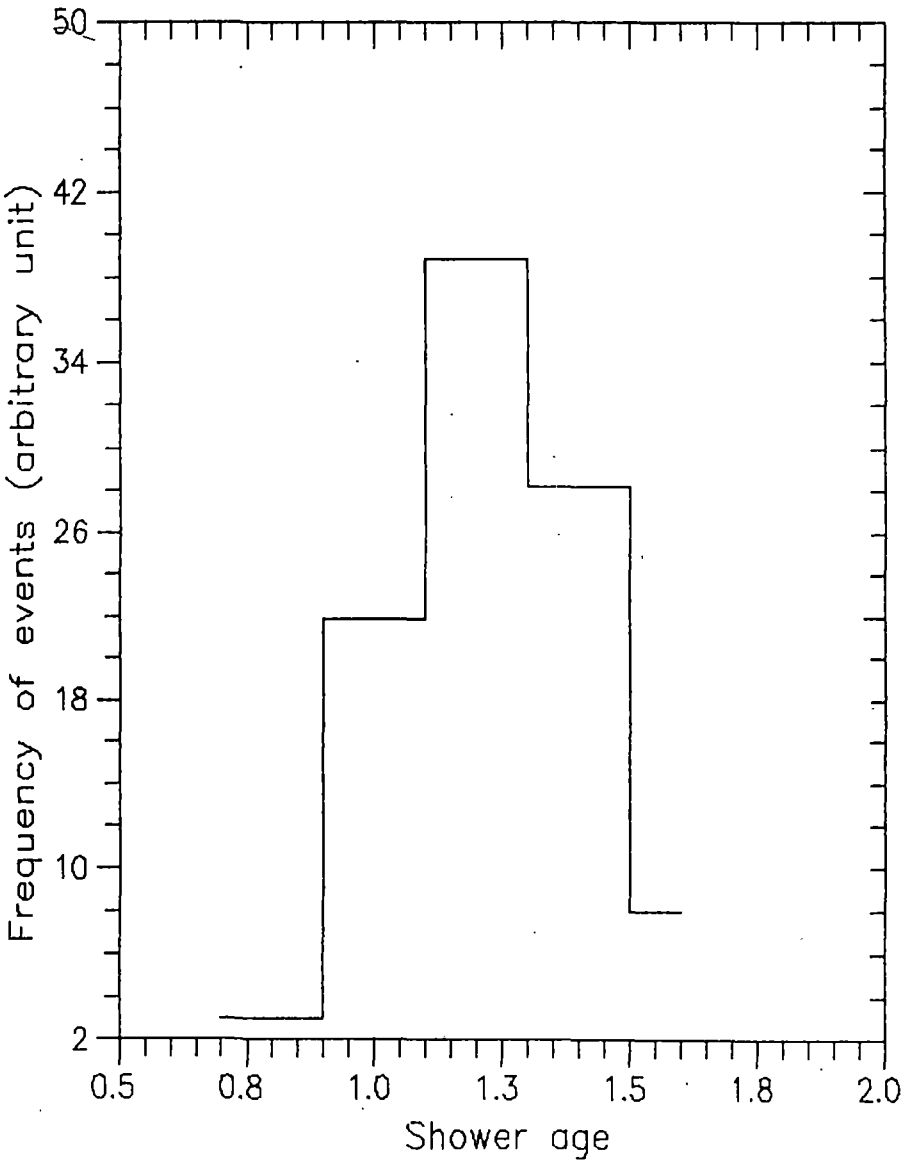

Fig.3.2. Frequency distribution of shower age of the observed shower events

For each shower of fixed size (N_e) and age (s) the mean energy of the primary particle (proton) (E_o) was obtained with a maximum error of 10% (which includes fluctuation in EAS development and the error in shower size measurement) from the energy scale established on the basis of hybrid Monte Carlo model (Trzupek et al [1]) for EAS at sea-level as given by

$$E_o(eV) = 3.03 \times 10^{10} \times N_e^{0.87} \quad \text{---------- (3.1)}$$

The mean primary energy was also obtained from the results of Monte Carlo simulations of EAS (Wrotniak and Yodh [2]) on the basis of different interaction models. For proton initiated shower and for the nuclear interaction model M-F00 , the relation between primary energy and shower size at sea-level is

$$E_o(eV) = 4.58 \times 10^{10} \times N_e^{0.84} \quad \text{---------- (3.2)}$$

In the analysis of the present experiment eqn.3.1 has been used to find out the primary energy from shower size.

3A.2. Radial distribution of electrons:

In the first step of the shower processing , the shower size N_e, the shower core Xo, Yo and the shower age s for each shower event are determined by fitting the measured particle densities to the fitting function (Hillas [3] function) by the chi-square minimisation procedure . Showers over the size range 10^4 - 2.5 x 10^6 particles are then divided into 8 groups with the size bins (1-2)x10^4 , (2-4)x10^4 , (4-8)x10^4 , (0.8-1.6)x10^5 , (1.6-3.2)x10^5 , (3.2-6.4)x10^5 , (0.64-1.28)x10^6 ,(1.28-2.56)x10^6 and for each group the whole radial range 0-45 m is again subdivided into 8 radial groups with distance bins (0-4)m ,(4-8)m ,(8-12)m ,(12-16)m ,(16-20)m ,(20-25)m ,(25-35)m , (35-45)m . The mean shower size , mean shower age for every shower size bin and mean core distances of different distance bins for a particular shower size bin are then calculated . For a particular shower size bin the mean electron density in a distance bin is determined following the relation

$$\Delta_e = 1/n \sum_i \Delta_{ei} \quad \text{----------(3.3)}$$

where n is the number of showers in that shower size bin as well as the distance bin. The transition effect arising from multiplication or absorption (absorption is predominant over multiplication)of shower particles in the finite thickness of a plastic scintillator in a density detector of the EAS array is taken into account and is corrected by using the relation as given by Asakimori et al [4] as

$$\Delta_c = \Delta_e(1.192 - 0.136 \log r)$$

where Δ_c and Δ_e are the corrected and measured densities respectively and r is the distance of the detector from the shower core.

The observed radial distribution of electrons for showers of sizes 1.09×10^5 , 4.48×10^5 and 1.79×10^6 along with the curves obtained from the Hillas function are shown in figs. 3.3 , 3.4 and 3.5. It is seen from the figures that the observed radial distributions up to the core distance of 45m are in good agreement with those predicted by Hillas et al [3].

3A.3.Measurement of muon density:

In the present experiment two identical magnetic spectrograph units separated by a distance of 4m are operated with the air shower array to detect the muon component in EAS.

The density of muons is calculated in the following way. The average muon density in near vertical showers as a function of radial distance from the shower core for each of the various shower groups in the shower size range 1.52×10^4 - 1.79×10^6 particles is defined as

$$\rho_\mu(\geq E_\mu, N_e, r) = n_\mu(\geq E_\mu, N_e, r) / [N_t(N_e, r).A'] \text{ ---------- } (3.4)$$

where $n_\mu(\geq E_\mu, N_e, r)$ is the total number of muons recorded in a particular distance interval (r) for a particular shower size (N_e) in a certain period of time above the threshold energy ($\geq E_\mu$) , N_t (N_e,r) represents the total number of showers of size N_e at the distance interval (r) recorded at the same time and A' is the effective area of the muon detector.The effective area of the muon detector A' is nearly same for all the observed muons since the maximum projected angle by the magnetic spectrograph is very low (i.e, near vertical)

3A.4. Radial distribution of muons:

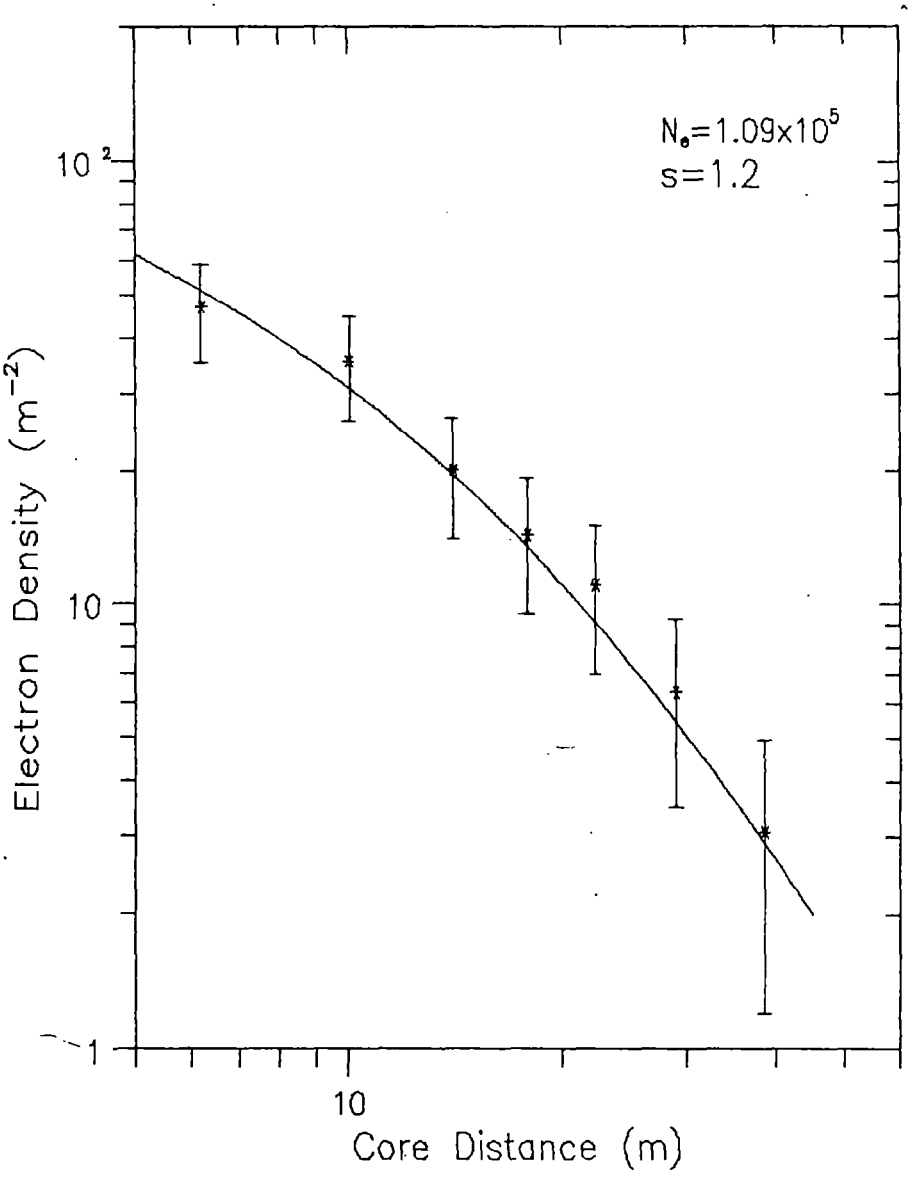

Fig.3.3. Observed radial distribution of EAS electrons compared with the Hillas function (solid line) for shower size 1.09×10^5 and shower age 1.2

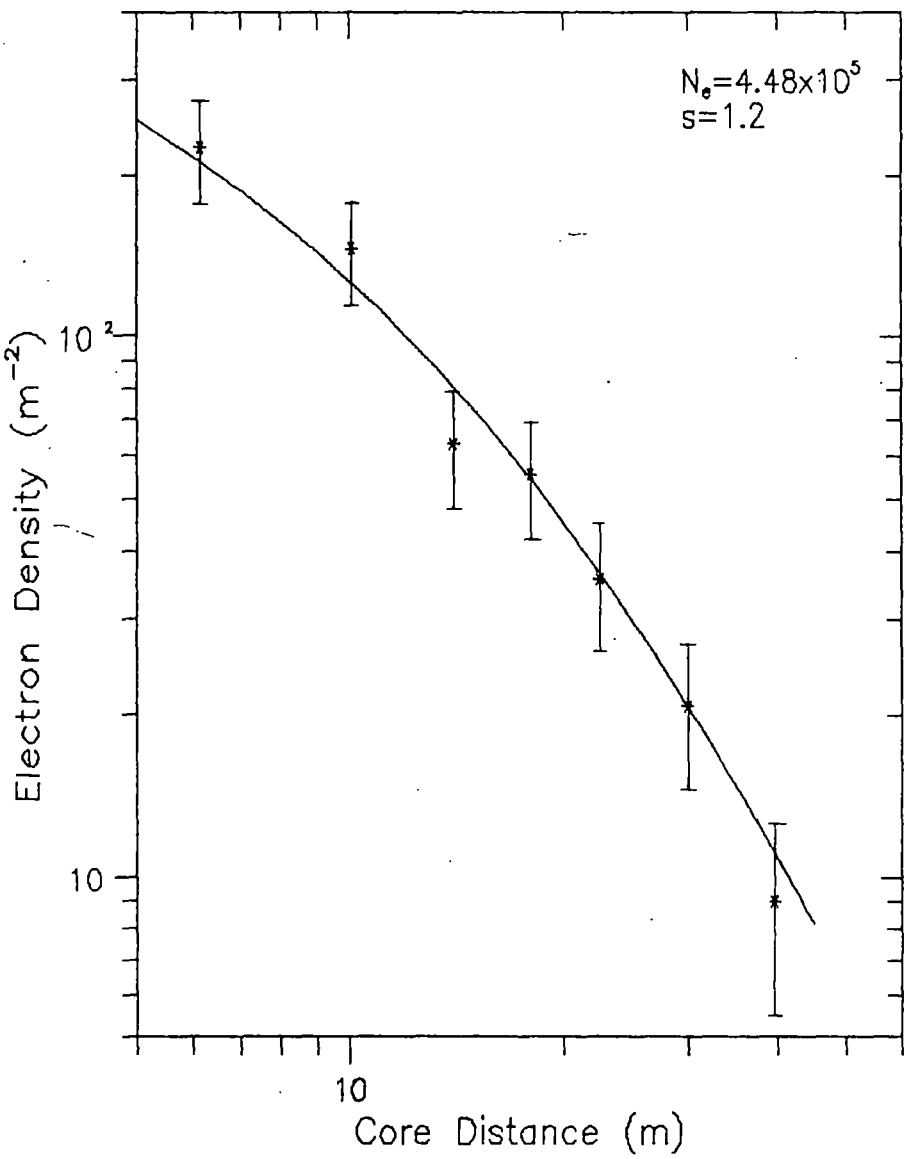

Fig.3.4. Observed radial distribution of EAS electrons compared with the Hillas function (solid line) for shower size 4.48×10^5 and shower age 1.2

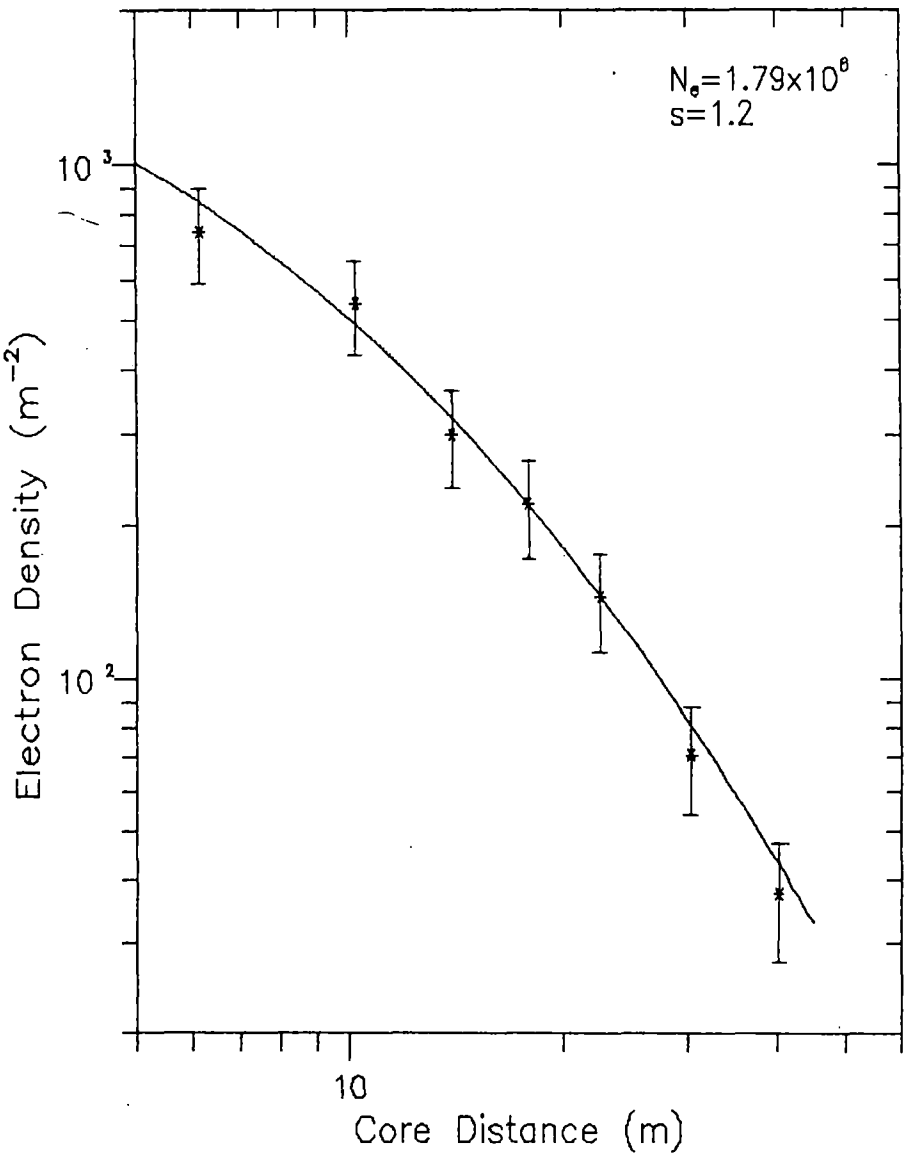

Fig.3.5. Observed radial distribution of EAS electrons compared with the Hillas function (solid line) for shower size 1.79×10^6 and shower age 1.2

In a particular shower group the muons are divided into groups in terms of chosen threshold energies ($\geq E_\mu$) and then each group is distributed into a number of bins with respect to radial distances from the shower core to determine the average muon density as a function of radial distance and threshold energy.

The density of muons for $E_\mu \geq 2.5$, 5 , 10 , 20 , 50 , 75 and 100 GeV are calculated using the equation (3.4) . The observed radial distribution of muons for different muon threshold energies and shower sizes are fitted to a relation of the form

$$\rho_\mu(\geq E_\mu, N_e, r) = A \, .r^{-\alpha(\geq E\mu)}.\exp(-r/r_o) \text{ --------- } (3.5)$$

where A , α and r_o are the fitting parameters . The values of A and α for different shower sizes and different threshold energies are given in table 3.1.

TABLE - 3.1

Values of α and A at different shower sizes and muon threshold energies

Muon threshold energies($\geq E_\mu$) in GeV	Shower sizes	α	A
2.5	3.15×10^4	0.337 ±0.067	0.441 ± 0.083
	5.97×10^4	0.344 ±0.067	0.702 ± 0.130
	1.09×10^4	0.373 ±0.068	1.157 ± 0.219
	2.21×10^5	0.392 ±0.067	1.975 ± 0.369
	4.48×10^5	0.434 ±0.066	3.597 ± 0.665
	9.02×10^5	0.386 ±0.069	4.923 ± 1.023
	1.79×10^6	0.339 ±0.085	6.548 ± 1.744
5	3.15×10^4	0.360 ± 0.065	0.421 ± 0.076
	5.97×10^4	0.368 ± 0.070	0.673 ± 0.132
	1.09×10^4	0.422 ± 0.066	1.179 ± 0.217
	2.21×10^5	0.444 ± 0.066	2.040 ± 0.377
	4.48×10^5	0.468 ± 0.068	3.519 ± 0.676

	9.02×10^5	0.456 ± 0.064	5.391 ± 0.986
	1.79×10^6	0.386 ± 0.087	6.232 ± 1.697
10	3.15×10^4	0.471 ± 0.070	0.486 ± 0.095
	5.97×10^4	0.483 ± 0.067	0.784 ± 0.145
	1.09×10^5	0.510 ± 0.063	1.273 ± 0.222
	2.21×10^5	0.538 ± 0.062	2.203 ± 0.384
	4.48×10^5	0.564 ± 0.062	3.827 ± 0.667
	9.02×10^5	0.566 ± 0.070	6.117 ± 1.230
	1.79×10^6	0.497 ± 0.089	7.595 ± 2.115
20	5.97×10^4	0.572 ± 0.074	0.763 ± 0.158
	1.09×10^5	0.599 ± 0.065	1.280 ± 0.230
	2.21×10^5	0.664 ± 0.064	2.454 ± 0.438
	4.48×10^5	0.730 ± 0.063	4.782 ± 0.852
	9.02×10^5	0.740 ± 0.073	7.772 ± 1.702
	1.79×10^6	0.747 ± 0.076	12.214 ± 2.778
50	5.97×10^4	0.808 ± 0.080	0.922 ± 0.205
	1.09×10^5	0.848 ± 0.077	1.524 ± 0.327
	2.21×10^5	0.892 ± 0.075	2.707 ± 0.566
	4.48×10^5	0.942 ± 0.072	4.932 ± 1.002
	9.02×10^5	0.975 ± 0.077	8.693 ± 2.011
	1.79×10^6	0.970 ± 0.077	13.342 ± 3.078
75	5.97×10^4	0.960 ± 0.078	0.989 ± 0.214
	1.09×10^5	1.014 ± 0.084	1.680 ± 0.393
	2.21×10^5	1.047 ± 0.080	2.953 ± 0.663
	4.48×10^5	1.098 ± 0.083	5.311 ± 1.242
	9.02×10^5	1.126 ± 0.073	9.115 ± 1.913
	1.79×10^6	1.101 ± 0.085	12.447 ± 3.176
100	1.09×10^5	1.110 ± 0.091	1.654 ± 0.417
	2.21×10^5	1.161 ± 0.081	3.051 ± 0.690
	4.48×10^5	1.233 ± 0.083	5.679 ± 1.316

9.02×10^5	1.286 ± 0.083	10.794 ± 2.552
1.79×10^6	1.257 ± 0.082	14.455 ± 3.557

The radial distribution of muons along with the curves obtained from the fitting function (3.5) at various shower sizes for each of the muon threshold energies from 2.5 to 100 GeV are shown in figs. 3.6 to 3.11.

Some observed results on energy spectra of muons along with those obtained from Khrenov and Linsley [5] function are also shown in figs. 3.12 , 3.13 , 3.14 and 3.15.and it is seen that the observed energy spectra of muons are in good agreement with the results of Khrenov and Linsley.

3A.5. Comparison of radial distribution of muons with calculations:

The observed radial distribution of muons for $N_e=9.02\times10^5$ and $E\mu \geqslant 10$ GeV are compared in fig.3.16 with the calculated results of Greisen [6] distribution function as given by

$$\rho_\mu(\geqslant E_\mu, N_e, r)=(14.4.r^{-0.75})(N_e/10^6)^{0.75}(1+r/320)^{-2.5}\,(51/(E_\mu+50))(3/(E_\mu+12))^{0.14r^{0.37}} \quad \text{---------- (3.6)}$$

and the results of Khrenov and Linsley [5] distribution function as given by

$$\rho_\mu(\geqslant E_\mu, N_e, r) = \{5\times10^3/(E_\mu+250)^{1.4}\}.r^{-0.55\eta^{0.1}}\,\psi^{0.07}\exp(-\eta^{0.62}\, r/80)\psi^{0.78} \quad \text{---------- (3.7)}$$

where $\eta = (E_\mu+2)/12$ and $\psi = N_e/(2\times10^5)$.

Equation (3.6) is valid for N_e in the range 10^5-10^8 , $E_\mu \leqslant 500$ GeV and equation (3.7) is valid for N_e in the range 3×10^4-10^6 , E_μ in the range 50 GeV- 6×10^3 GeV. Fig.3.16 shows that the observed radial muon density distributions are in good agreement with the distributions of Khrenov and Linsley but are flatter than Greisen's prediction.

3A.6.Comparison of radial distribution of muons with other experimental data:

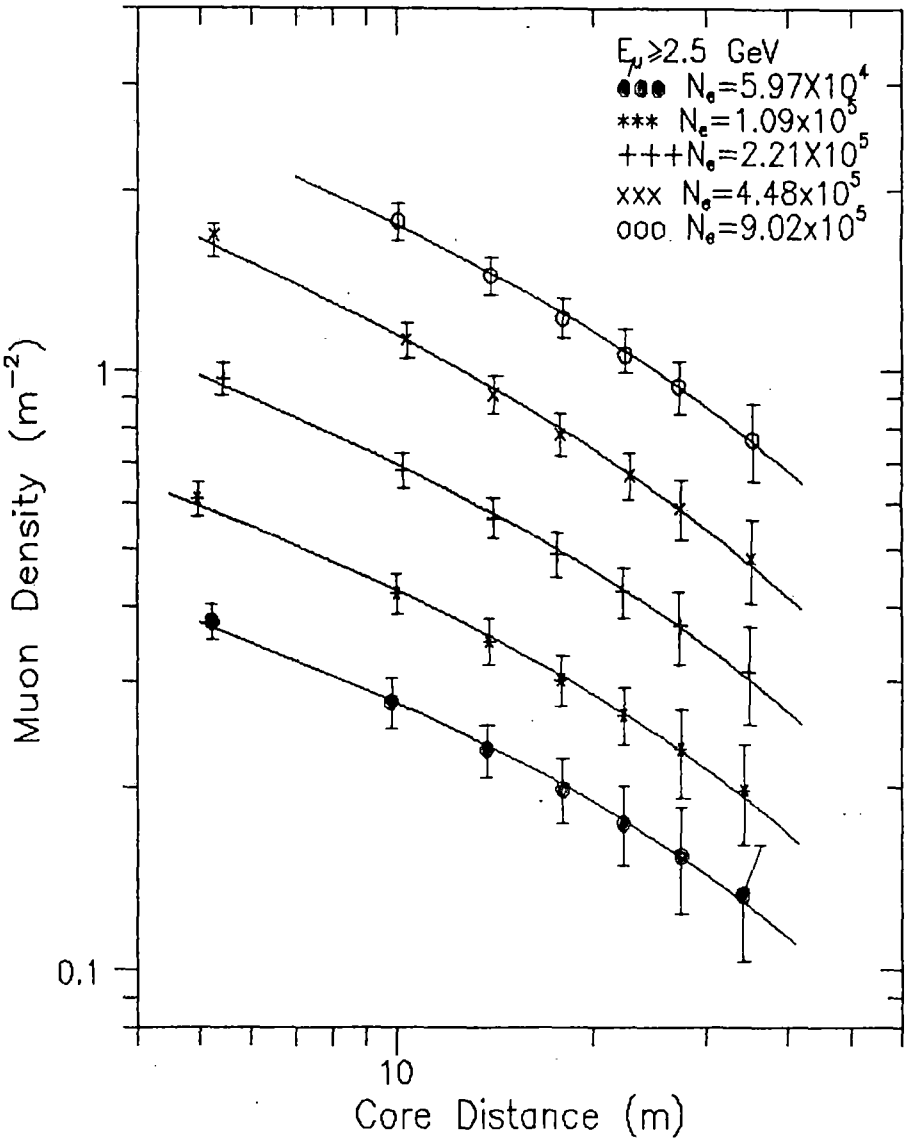

Fig.3.6. Observed radial distribution of EAS muons for muon threshold energy 2.5 GeV and for various shower sizes . The least-squares fit to the data are shown as solid lines.

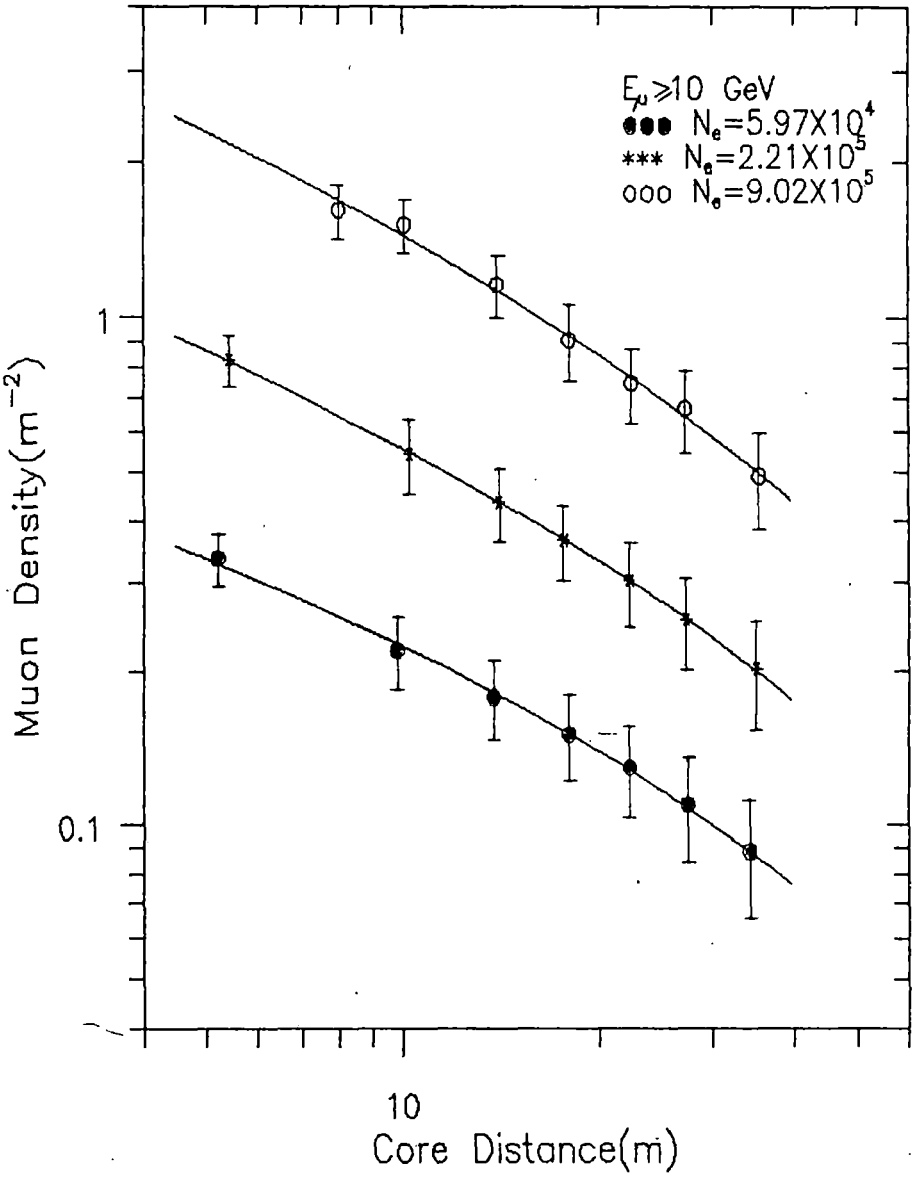

Fig.3.7. Observed radial distribution of EAS muons for muon threshold energy 10 GeV and for various shower sizes . The least-squares fit to the data are shown as solid lines.

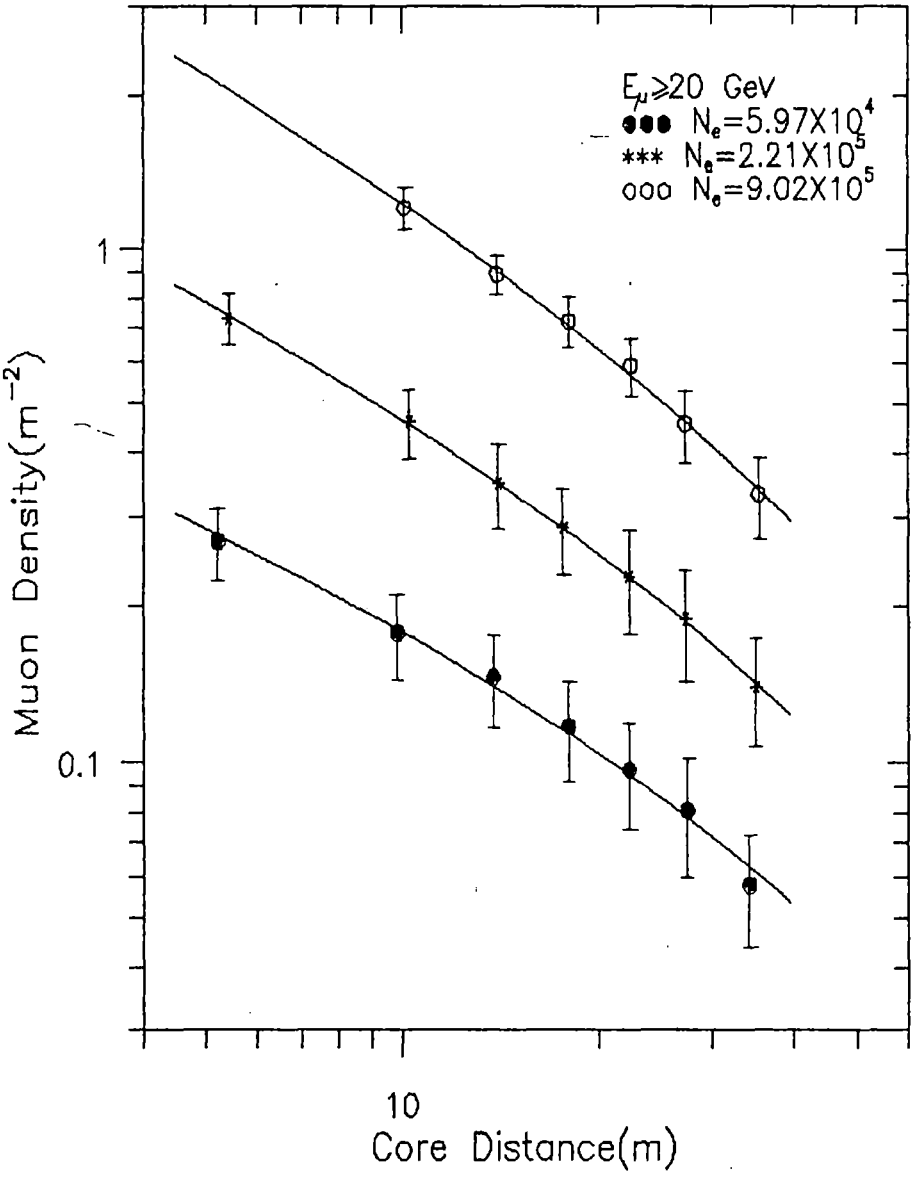

Fig.3.8. Observed radial distribution of EAS muons for muon threshold energy 20 GeV and for various shower sizes . The least-squares fit to the data are shown as solid lines.

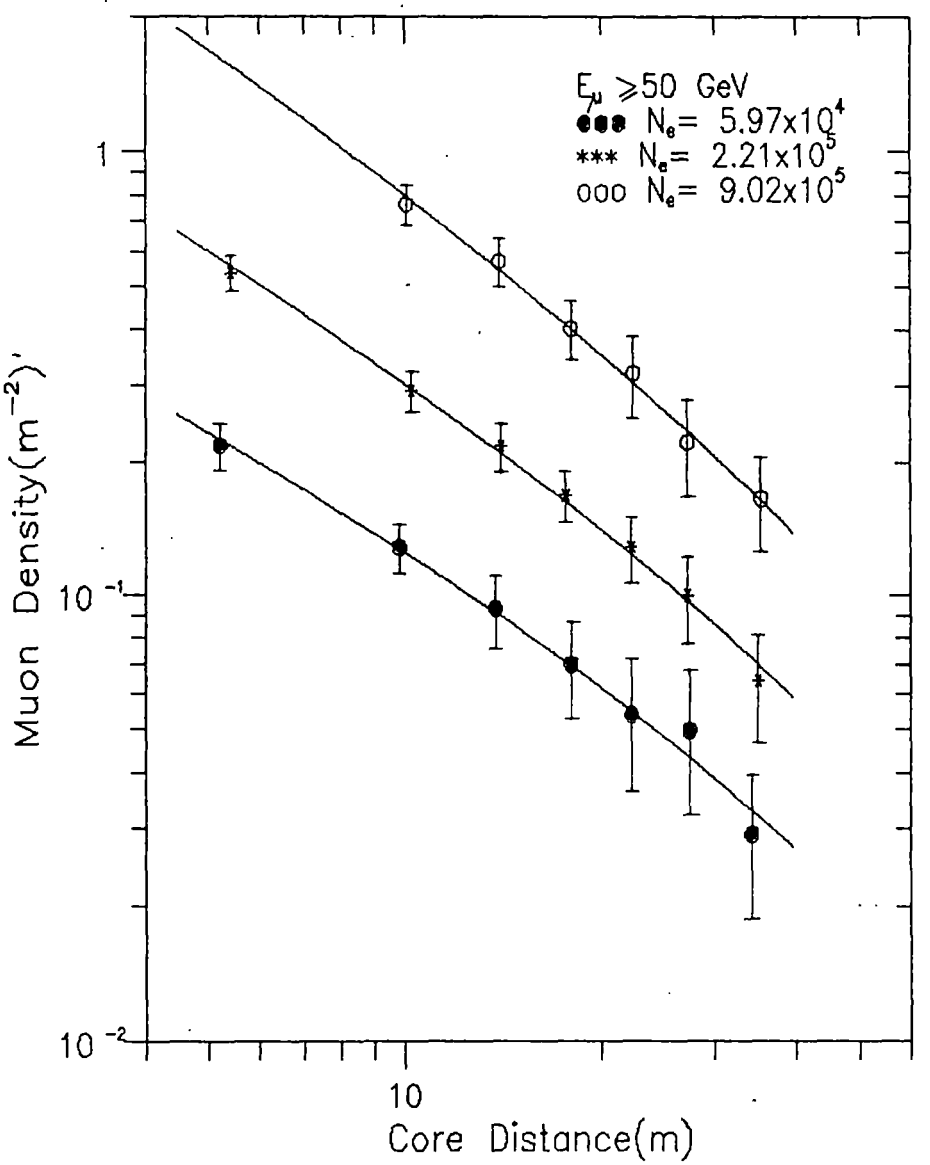

Fig.3.9. Observed radial distribution of EAS muons for muon threshold energy 50 GeV and for various shower sizes . The least-squares fit to the data are shown as solid lines.

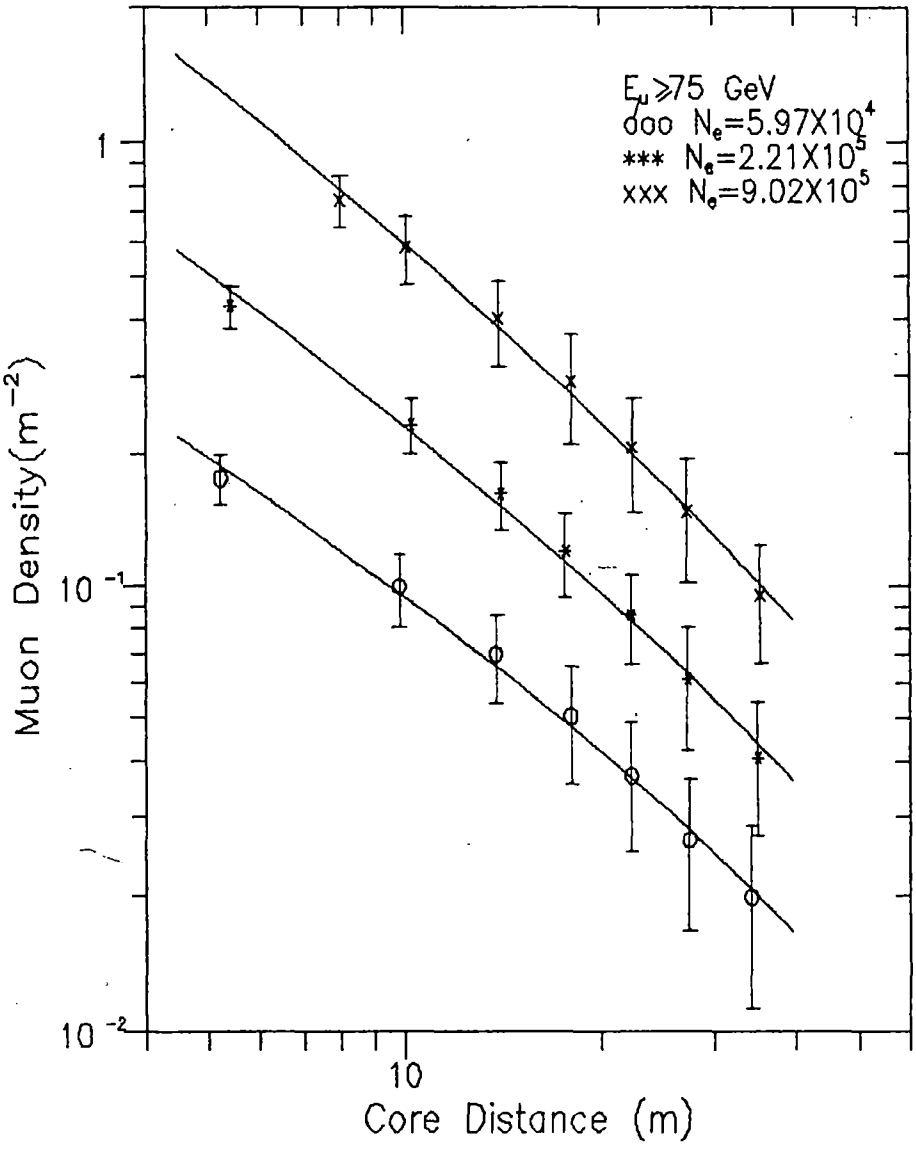

Fig.3.10. Observed radial distribution of EAS muons for muon threshold energy 75 GeV and for various shower sizes . The least-squares fit to the data are shown as solid lines.

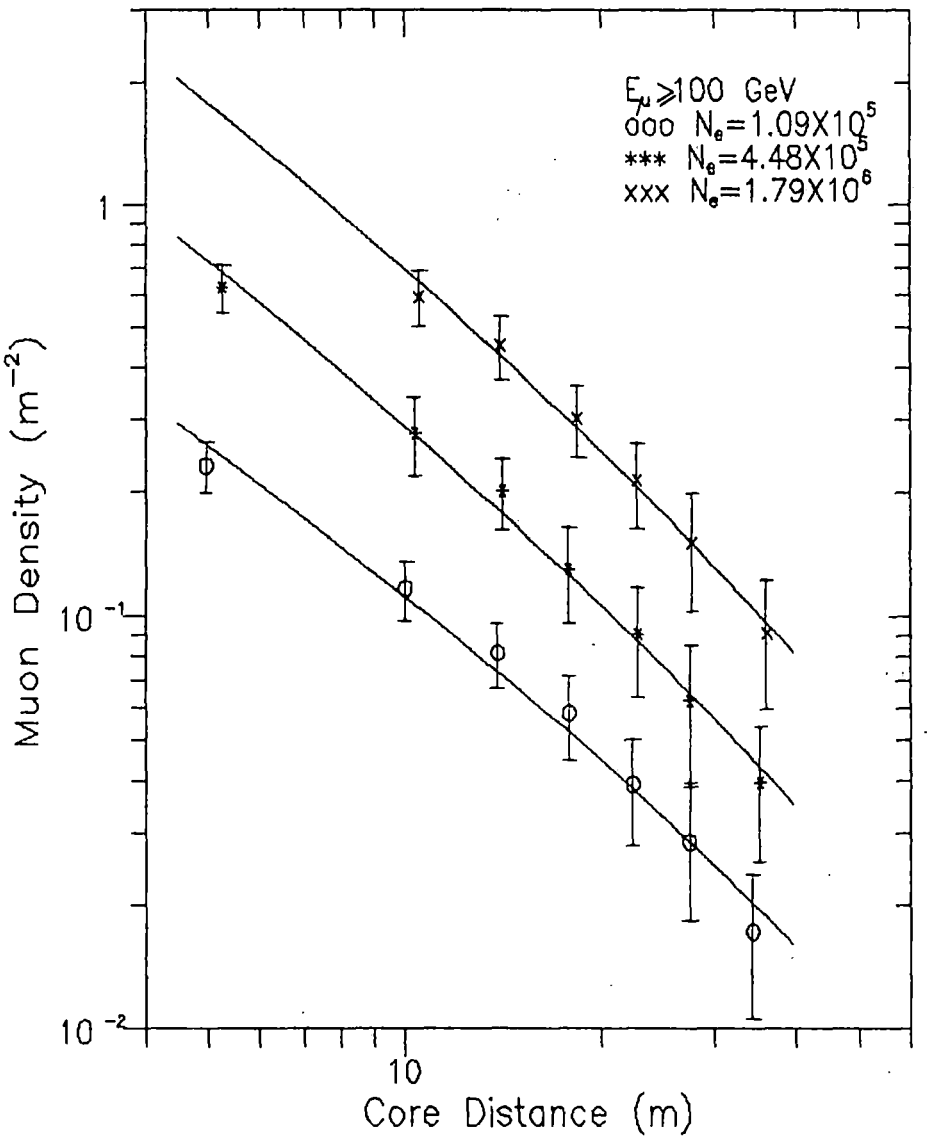

Fig.3.11. Observed radial distribution of EAS muons for muon threshold energy 100 GeV and for various shower sizes . The least-squares fit to the data are shown as solid lines.

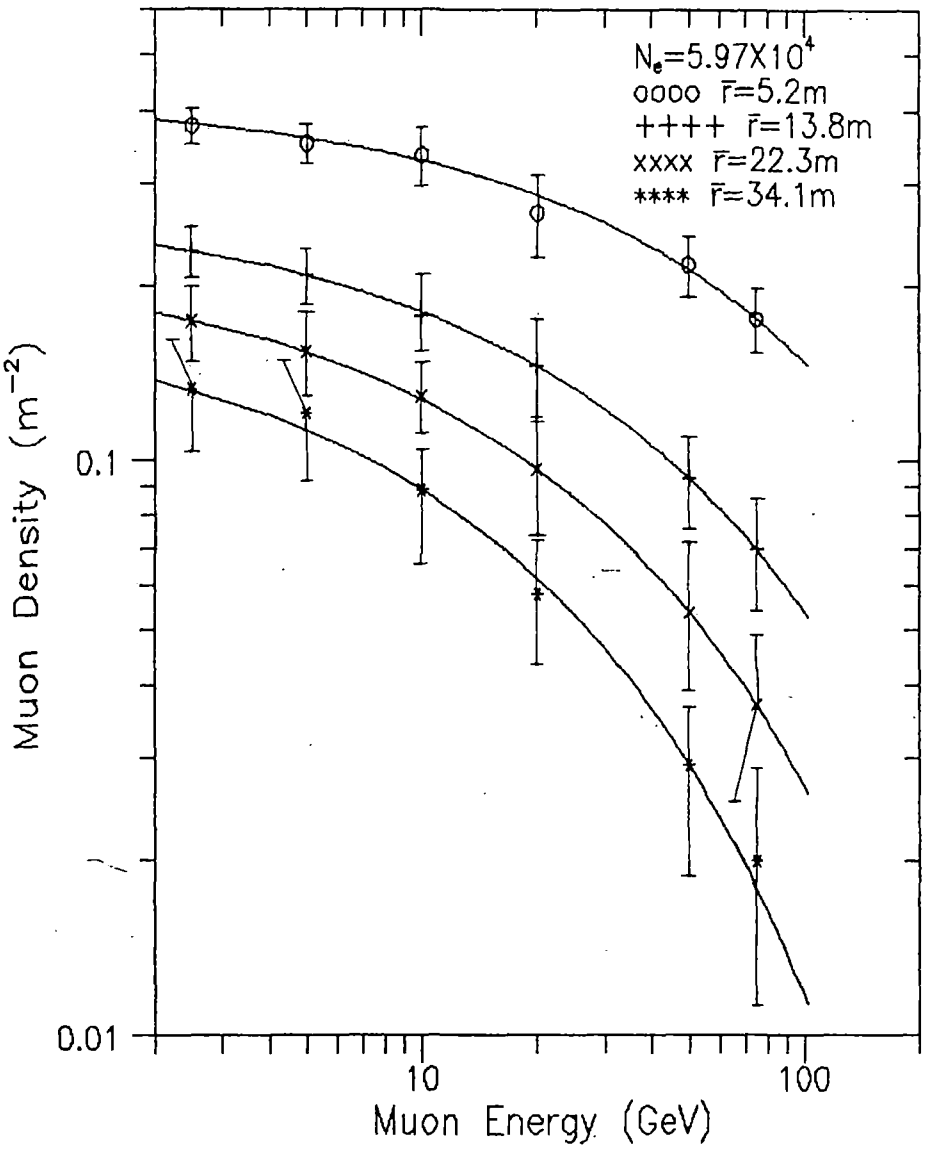

Fig.3.12. Variation of muon density with muon energy at various radial distances.

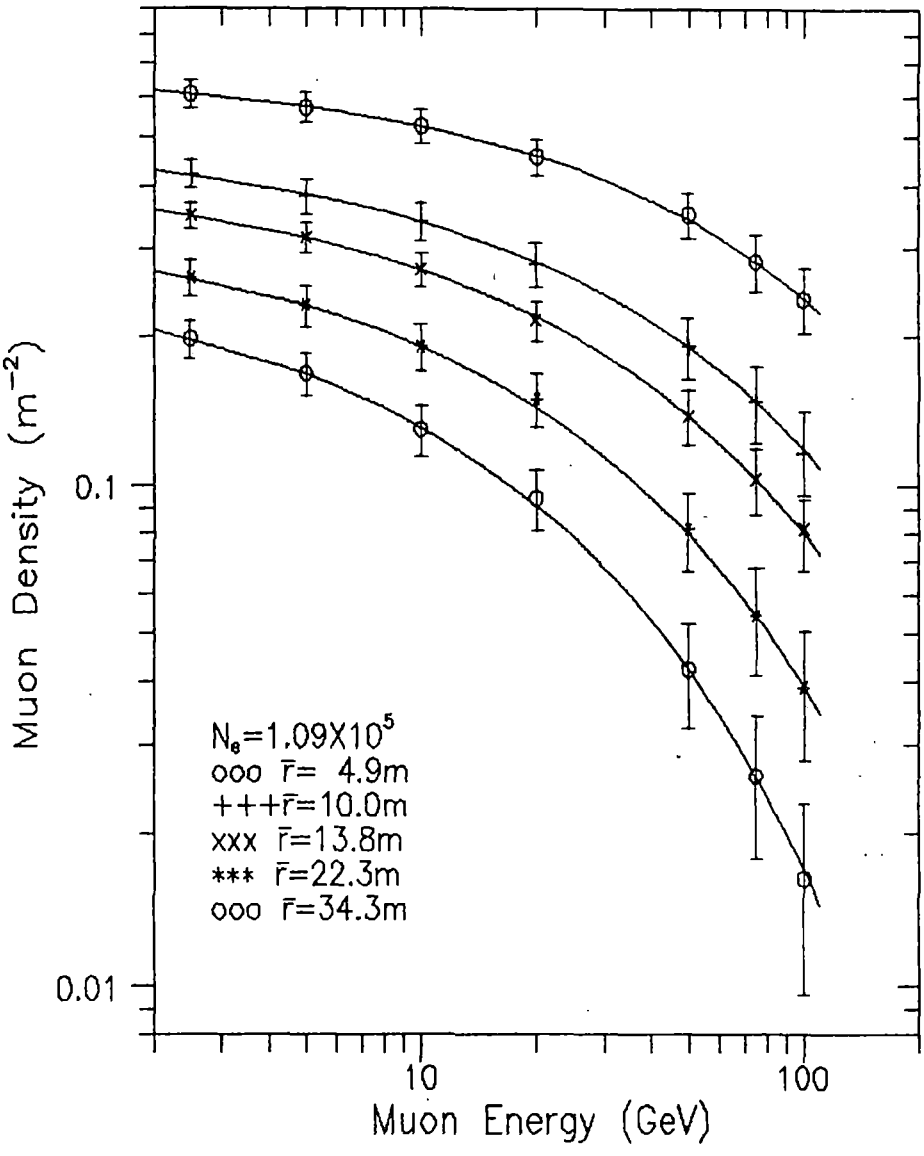

Fig.3.13. Variation of muon density with muon energy at various radial distances.

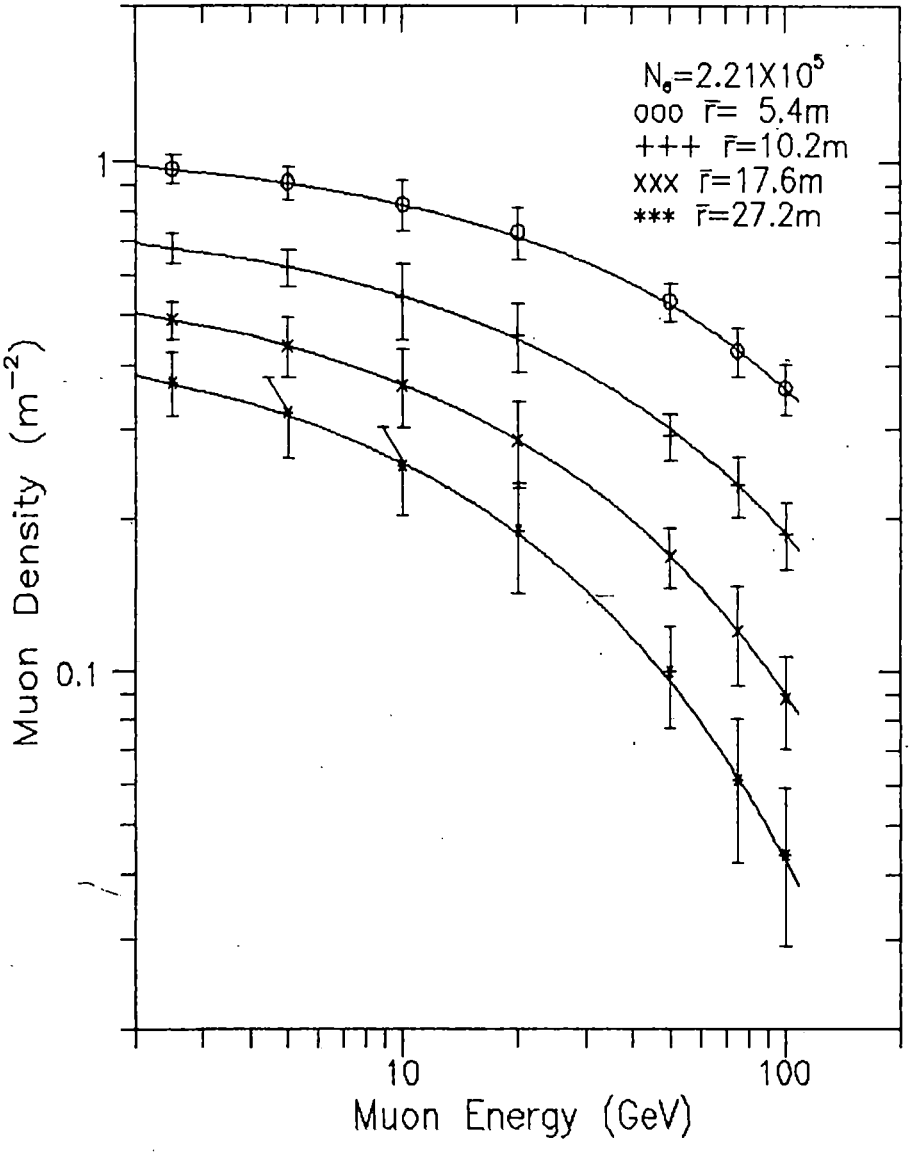

Fig.3.14. Variation of muon density with muon energy at various radial distances.

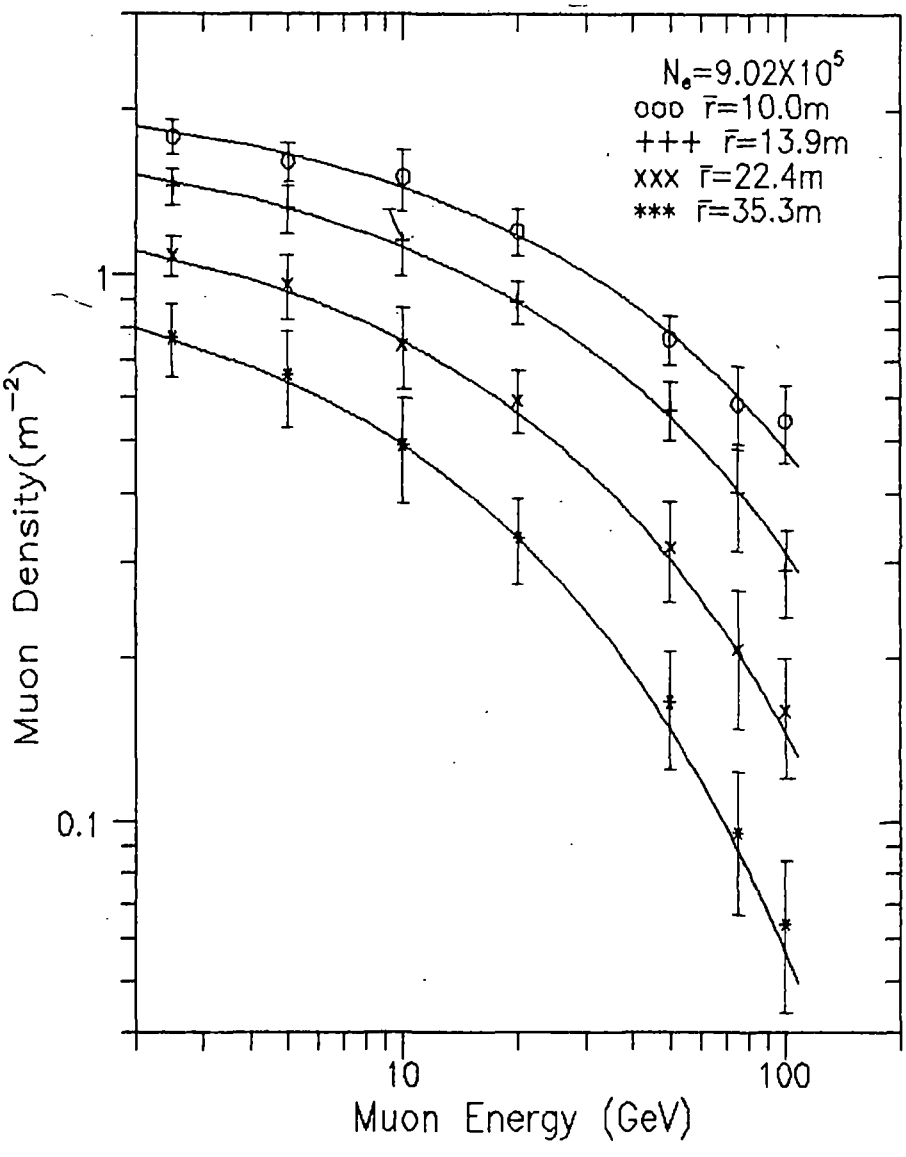

Fig.3.15. Variation of muon density with muon energy at various radial distances.

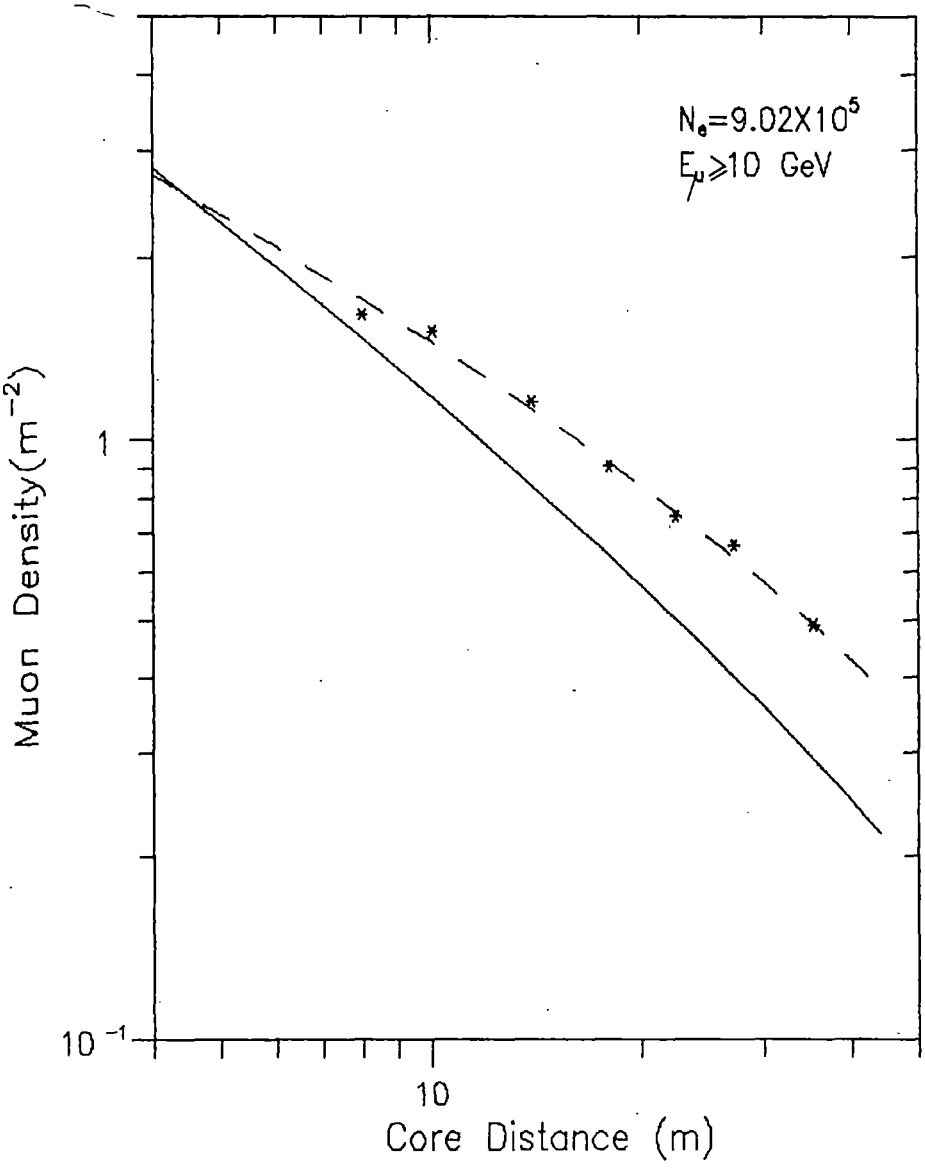

Fig.3.16. Observed radial muon density distribution along with the distributions using Greisen function (solid line) and Linsley function (dashed line) for shower size 9.02x10^5 and muon threshold energy 10 GeV

The radial density distribution of muons obtained from the present experiment are shown along with the experimental results of Khrenov (1961) [7] ,Khrenov (1966) [8] and Earnshaw et al [9] in fig.3.17 for $E_\mu \geq 10$ GeV and $N_e \sim 10^6$. It is seen from the figure that the observed radial distribution of muons are in close agreement with the results of Khrenov (1961) and Earnshaw et al. In fig.3.18 we have compared our results on radial distribution of muons with the experimental results of Rada et al [10] and Atrashkevich et al [11] for $E_\mu \geq 50$ GeV and $N_e \sim 10^6$. The experimental data of Rada et al deviate from our data whereas our data show a good agreement with the experimental results of Atrashkevich et al (Moscow group). For the same shower size but for $E_\mu \geq 100$ GeV , our radial distribution of muons also agree with the experimental results of Vashkevich et al [12] (Moscow group) which is shown in fig.3.19.

3A.7. Comparison of the measured radial density distribution of muons with Monte Carlo simulation result:

The radial density distribution of muons obtained from the Monte Carlo simulation results of S.Mikocki et al [13] for primary proton and the measured radial muon density distribution for primary energy $\sim 10^{15}$ eV and $E_\mu \geq 10$ GeV are shown in fig.3.20.It is seen from fig.3.20 that the observed radial muon density distribution is flatter compared to the distribution for primary proton.

3A.8. Variation of muon density to electron density ratio as a function of radial distance :

The variation of muon density to electron density ratio as a function of radial distance for primary energy 1.3×10^{15} eV and for $E_\mu \geq 2.5$ GeV has been studied and compared with the calculated results of S.Mikocki et al [13] on the basis of Monte Carlo simulation technique for primary (proton) energy 10^{15} eV and for $E_\mu \geq 1$ GeV which is shown in fig.3.21.

3A.9. Variation of muon size (N_μ) with shower size (N_e) :

The total number of muons above the threshold energy E_μ in a shower of size N_e was calculated by using the relation

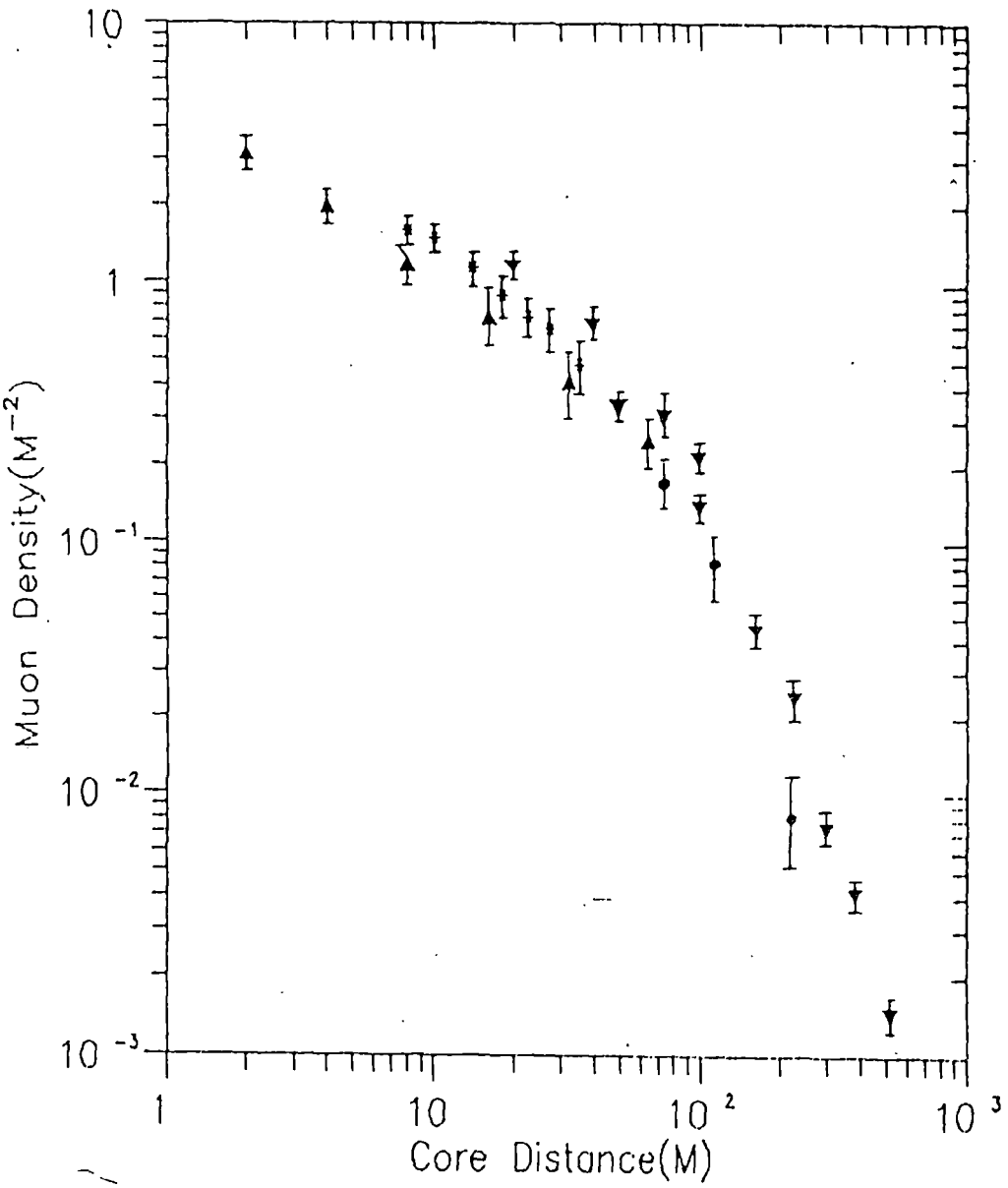

Fig.3.17. A comparison of the observed radial density distribution of muons of the present experiment (*) with the experimental results of Khrenov [5] (▲),Khrenov [6] (•) and Earnshaw et al [7] (▼) for $N_e \sim 10^6$ and $E_\mu \geqslant 10$ GeV

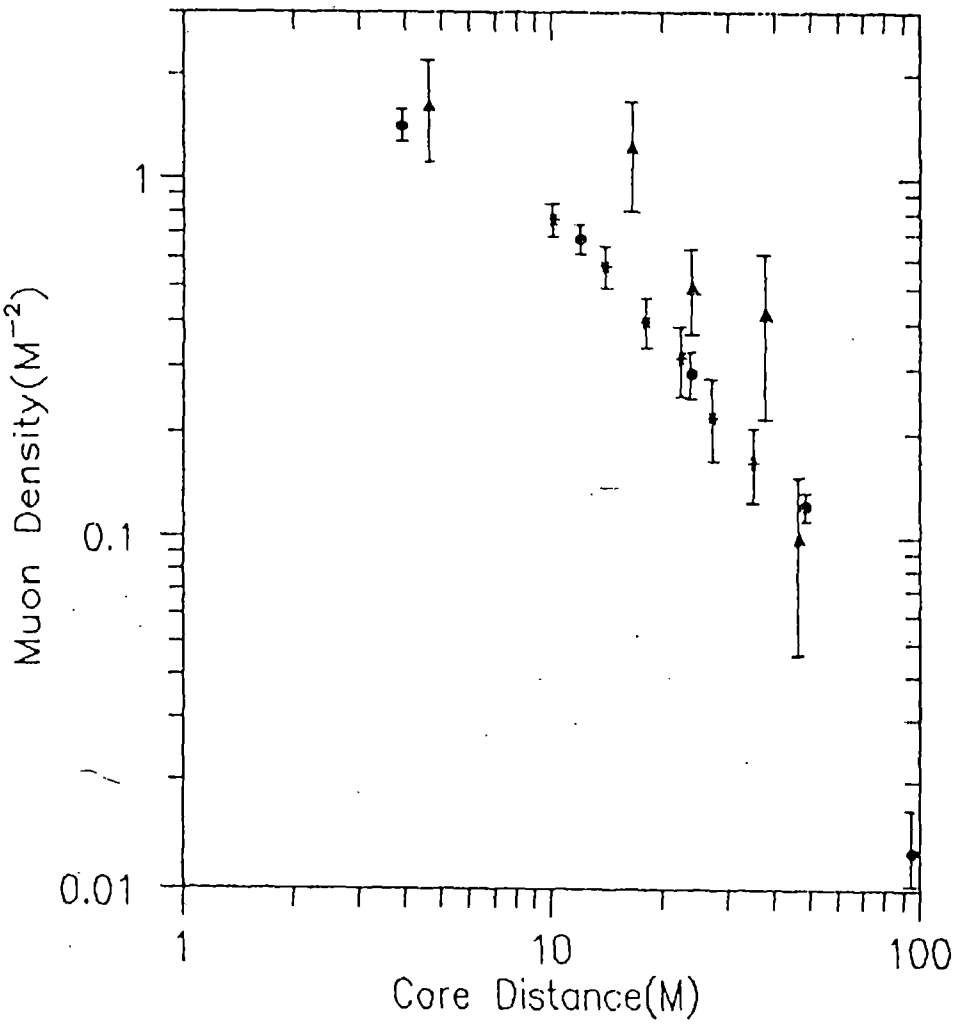

Fig.3.18. A comparison of the observed radial density distribution of muons of the present experiment (*) with the experimental results of Rada et al [8] (▲) and Atrashkevich et al [9] (•) for $N_e \sim 10^6$ and $E_\mu \geqslant 50$ GeV

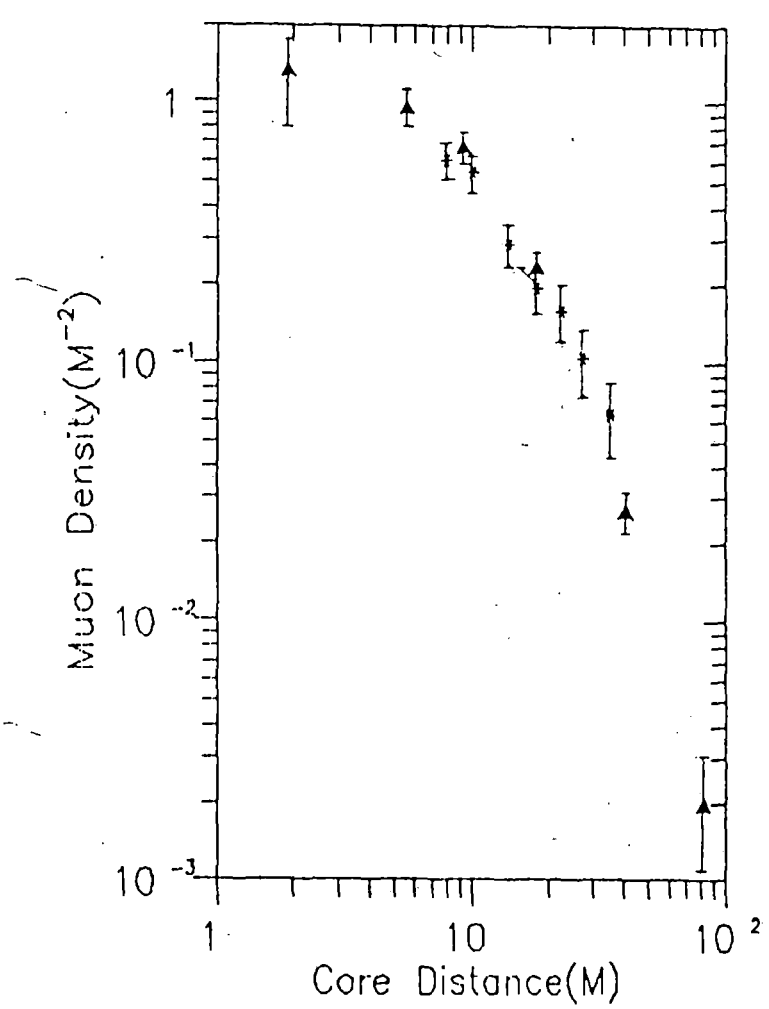

Fig. 3.19. A comparison of the observed lateral distribution of muons with the experimental results of Vashkevich et al [12] (▲) and the present experiment (*) for $N_e \sim 10^6$ and $E_\mu \geq 100$ GeV.

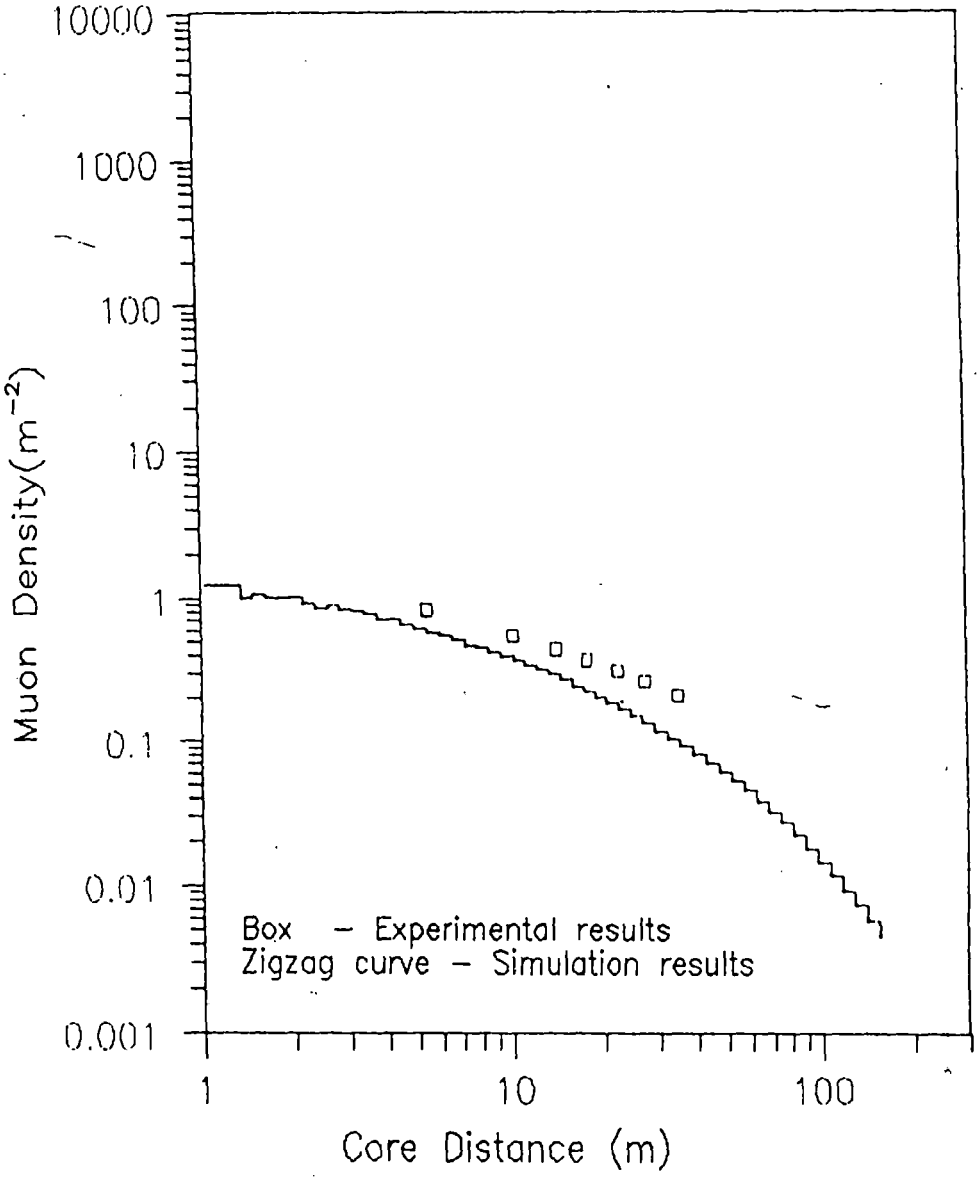

Fig.3.20. A comparison of the observed radial density distribution of muons for primary energy $\sim 10^{15}$ eV and muon threshold energy 10 GeV with the corresponding calculated results of Mikocki et al [13] for proton primary.

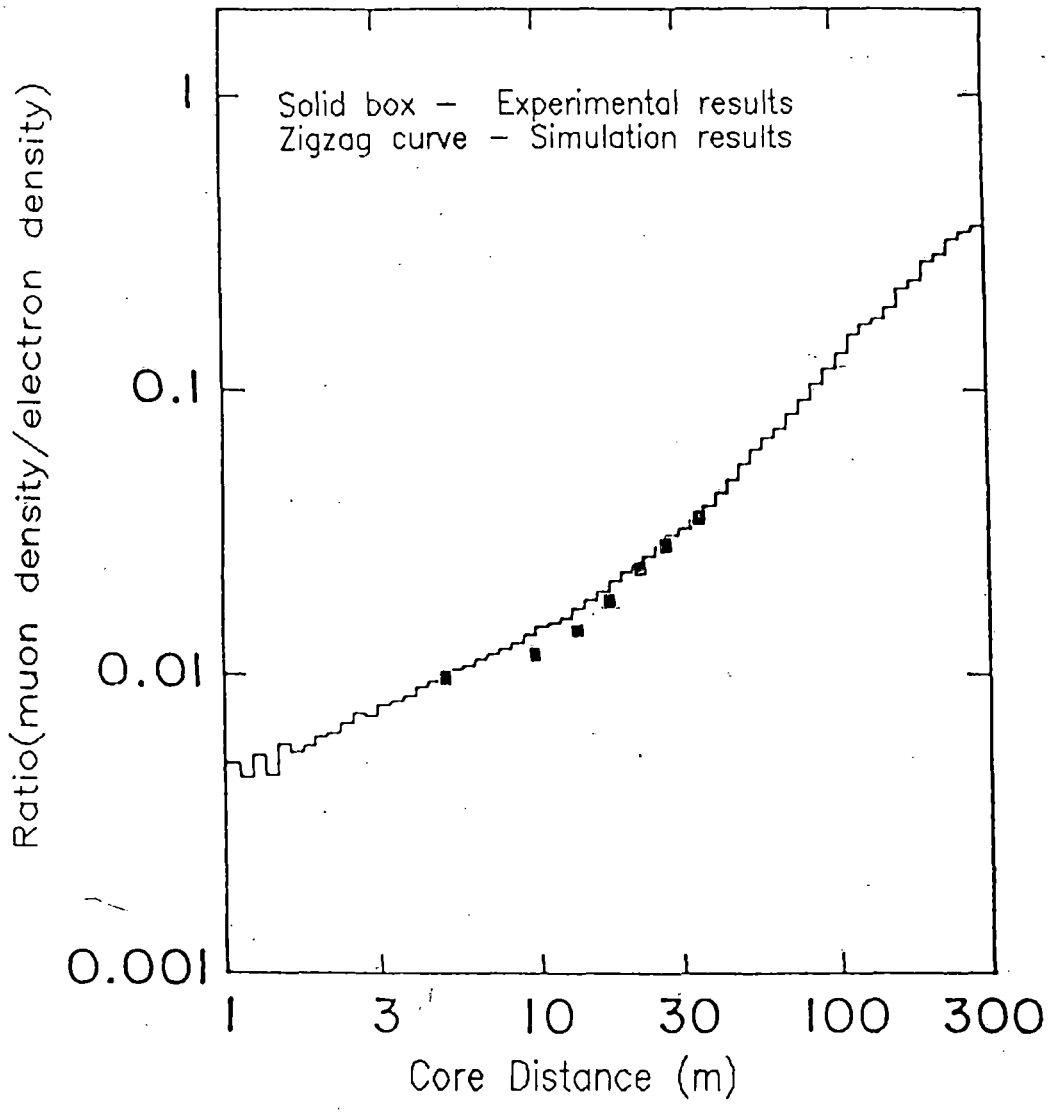

Fig.3.21. A comparison of the observed variation of muon density to electron density ratio as a function of radial distance for primary energy 1.3×10^{15} eV and muon threshold energy 2.5 GeV with the calculated results of Mikocki et al [13] for proton primary of energy 10^{15} eV and muon threshold energy 1 GeV.

$$N_\mu(\geq E_\mu, N_e) = \int_0^\infty \rho_\mu(\geq E_\mu, N_e, r)\, 2\pi r\, dr \quad \text{---------- (3.8)}$$

where $\rho_\mu(\geq E_\mu, N_e, r)$ is the density of muons with muon threshold energy $\geq E_\mu$ in a shower of size N_e at a distance r from the shower core and to calculate N_μ the functional form of ρ_μ as in equation (3.5) is considered . Then equation (3.8) becomes

$$N_\mu(\geq E_\mu, N_e) = 2\pi A \int_0^\infty r^{-\alpha+1} \exp(-r/r_o)\, dr \quad \text{---------- (3.9)}$$

The variation of muon size with shower size for muon threshold energies 2.5, 10, 20, 50 and 100 GeV are shown in fig.3.22 . The variation can be represented by a power law given by

$$N_\mu = AN_e^{\alpha} \quad \text{---------- (3.10)}$$

The values of α and A for different muon threshold energies are given in table 3.2.

TABLE - 3.2

Values of a and A for different muon threshold energies

Muon threshold energies ($\geq E_\mu$) in GeV	α	A
2.5	0.656	3.373
10	0.642	2.394
20	0.594	2.780
50	0.599	1.173
100	0.601	0.465

The observed variation of muon size with shower size for $E_\mu \geq 2.5$ GeV is compared with the Monte Carlo simulation results of Wrotniak and Yodh [14] calculated on the basis of nuclear interaction model M-F01 for proton primary and RM-F00 for iron primary for $E_\mu \geq 2$ GeV in fig.3.23.

Fig.3.24 shows the observed N_μ-N_e variation together with the calculated results of Hillas [15] at sea-level for muons of energy above 10 GeV . In this calculation the transport equations have been solved with the more accurate data from the accelerators by using the Feynman-Yan scaling model. The inelastic cross-

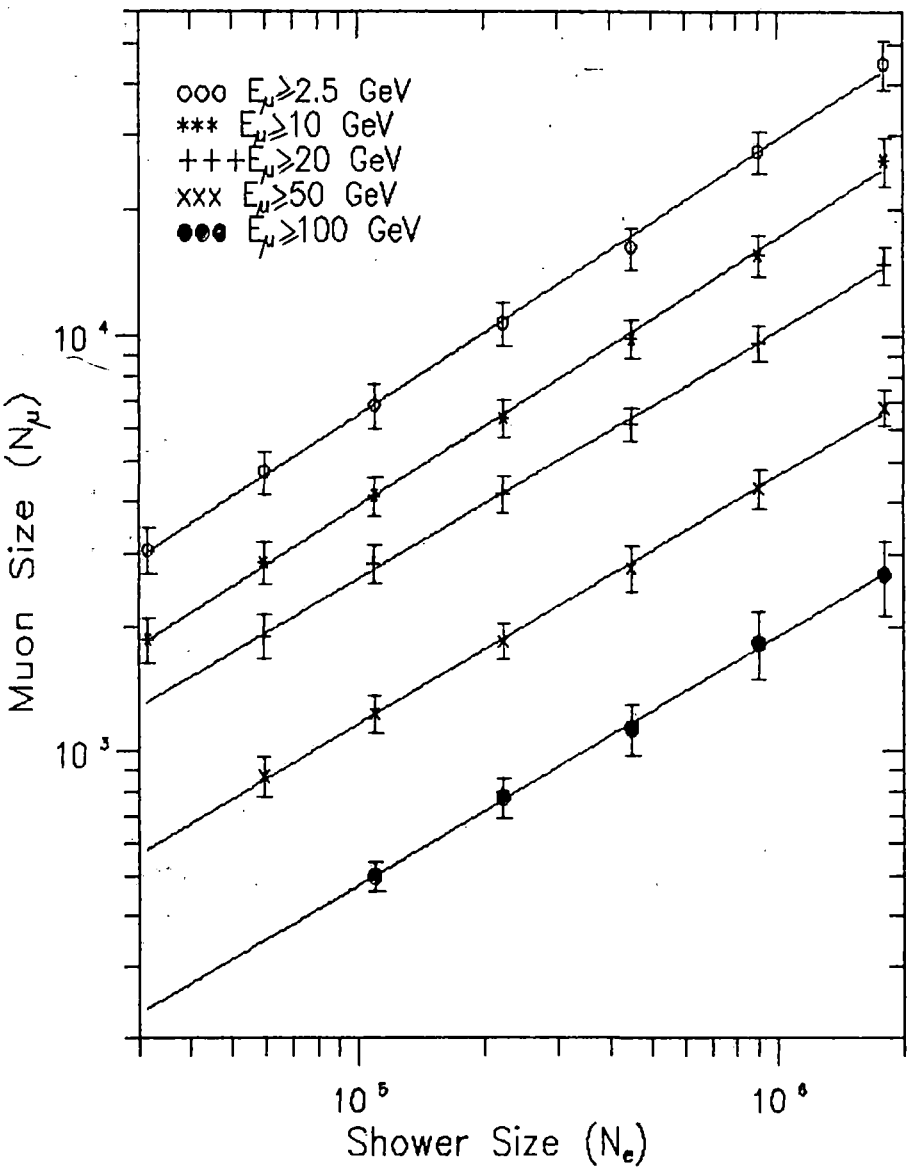

Fig.3.22. Variation of muon size with shower size for different muon threshold energies . The solid lines are the best fit to the data

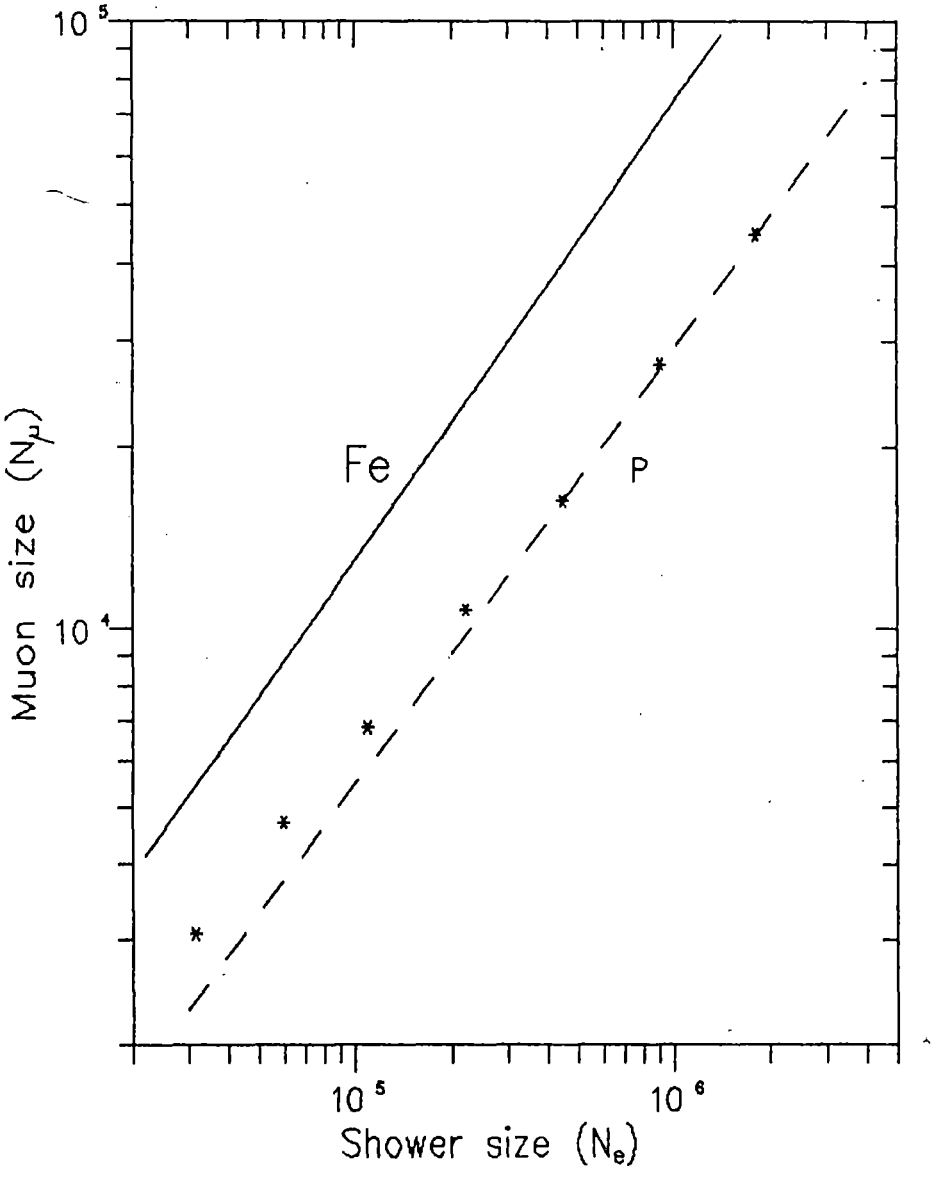

Fig.3.23. A comparison of the present results (star marks) of muon size dependence on shower size for $E_\mu \geqslant 2.5$ GeV with the corresponding Monte Carlo simulation results of Wrotniak and Yodh for $E_\mu \geqslant 2$ GeV using M-F01 model for proton primary (dashed line) and RM-F00 model for iron primary (solid line)

sections for collisions of hadron 'i' on nucleons are assumed to rise as follows at high energy :

$$\sigma_{in,inel} = \sigma_i [\ 1+0.0273\ u + 0.01u^2\ \theta(u)]\ ,$$

where $u=\ln(E/200GeV)$; $\theta(u) = 0$ if $u<0$, 1 if $u\geq 0$

For protons , pions and kaons σ_i is 32.2, 20.3 and 17.5 mb.The model calculations are shown as a stippled band , covering the range from proton primaries at the lower edge to iron primaries at the top, with solid circles (●) making the results of the mixed composition . From fig.3.24 it is seen that the observed N_μ–N_e variation for the shower size range 3.15 $x10^4$- 1.79 $x10^6$ particles is very close to the calculated results of Hillas for mixed composition.

Comparison have also been made of the experimentally observed N_μ-N_e variation with the Monte Carlo simulation results of Bourdeau et al [16] for $E_\mu \geq 10$ GeV in fig.3.25 . Scaling model is considered in the simulation work with particular attention to the following conditions and the consequences of their admixture

(i) rising p-air cross-section

(ii)shortened radiation length in e.m.cascades

(iii)mixed primary composition and modulation of the galactic confinement according to the Larmor radius of different nuclei.

It is seen from fig.3.25 that the primary composition in the shower size range 3.15 $x10^4$ - 1.79 $x10^6$ particles is neither purely proton nor iron rather mixed.

SECTION - 3B

In the previous section of this chapter the observed variations of total number of muons (N_μ) with shower size at different muon threshold energies have been studied and compared with different Monte Carlo simulation results . These comparisons seem to indicate that the composition of primary mass in the shower size range 3.15 $x10^4$ - 1.79 $x10^6$ particles is mixed .

Here the characteristics of the radial muon density distribution at fixed shower size and the variation of muon density with shower size at fixed radial distance for various muon threshold energies have been determined to draw conclusion about the change of the primary mass with the change of the energy of the primary particle in the knee energy region.

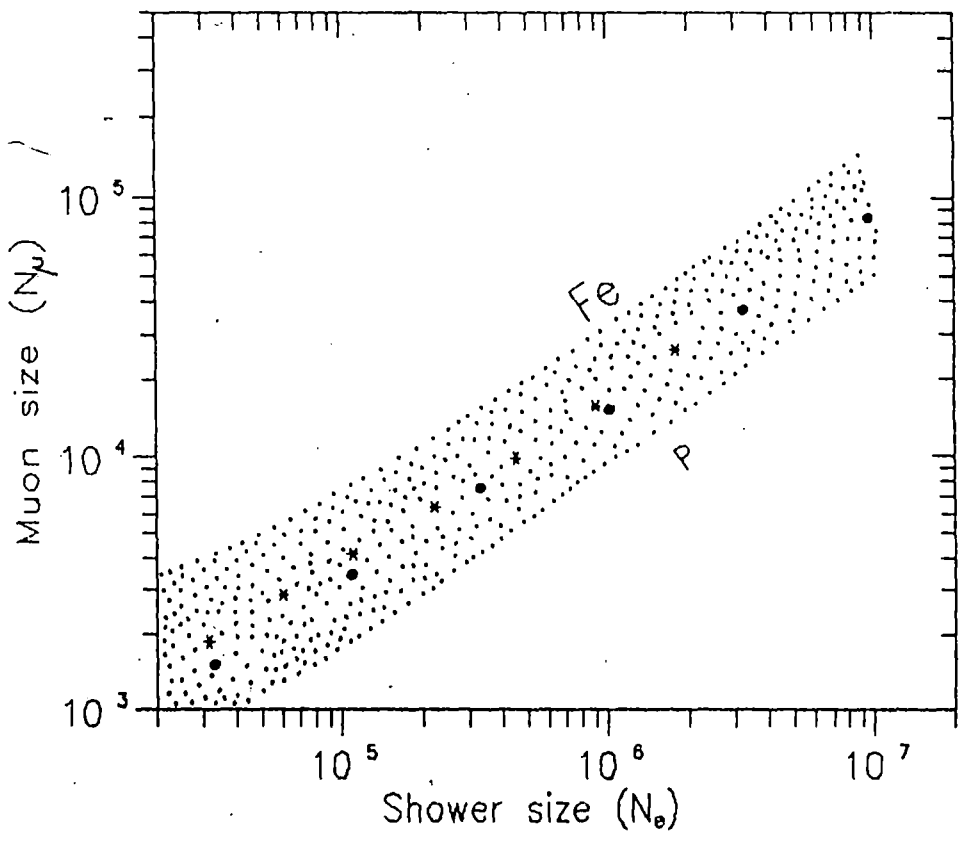

Fig.3.24. A comparison of the present results (*) of muon size dependence on shower size with the calculated results of Hillas [15] for $E_\mu \geq 10$ GeV

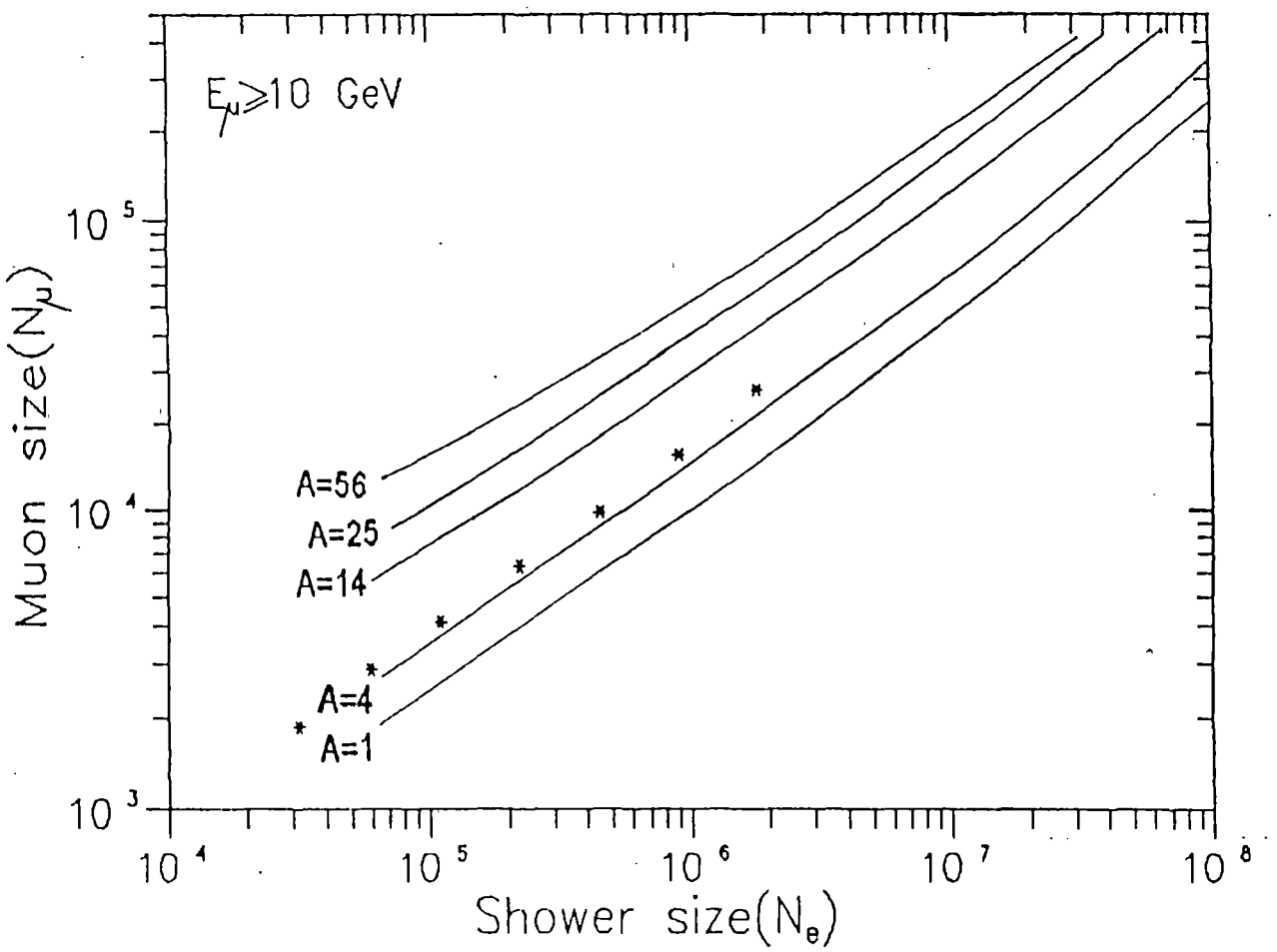

Fig.3.25. A comparison of the present results (*) of muon size dependence on shower size with the calculated results of Bourdeau et al [16] for $E_\mu \geq 10$ GeV and for different primary mass numbers

3B.1. The dependence of muon density on shower size :

The variation of muon density at fixed radial distances has been studied as a function of shower size at various muon threshold energies by assuming a dependence of the form given by

$$\rho_\mu(\geq E_\mu, r) \sim N_e^{\beta(E_\mu, r)} \qquad \text{---------- (3.11)}$$

The fit to the observed data has yielded the results shown in figs.3.26 , 3.27 , 3.28.It is seen that at a fixed muon threshold energy β decreases slowly with radial distance for all shower sizes in the range 3.15 $x10^4$ - 1.79 $x10^6$ particles and the trend of variation of β with radial distance is similar for all muon threshold energies .All these results together seem to indicate that the muon distribution function does not change with primary energy.The values of the exponent (β) obtained by fitting the observed data are given in table 3.3.

TABLE - 3.3

Values of the exponent (β) at different distance ranges for various muon energies

Muon energy (GeV)	β (for r=8-12m)	β(for r=30-40m)
2.5	0.692 ± 0.009	0.653 ± 0.012
10	0.699 ± 0.010	0.655 ± 0.013
50	0.661 ± 0.011	0.587 ± 0.021

3B.2. Muon density dependence on radial distance:

The measured radial distribution of muons in showers of various sizes can also be fitted to a relation of the form

$$\rho_\mu(\geq E_\mu, N_e, r) \sim r^{-\alpha(\geq E\mu)} \qquad \text{———————— (3.12)}$$

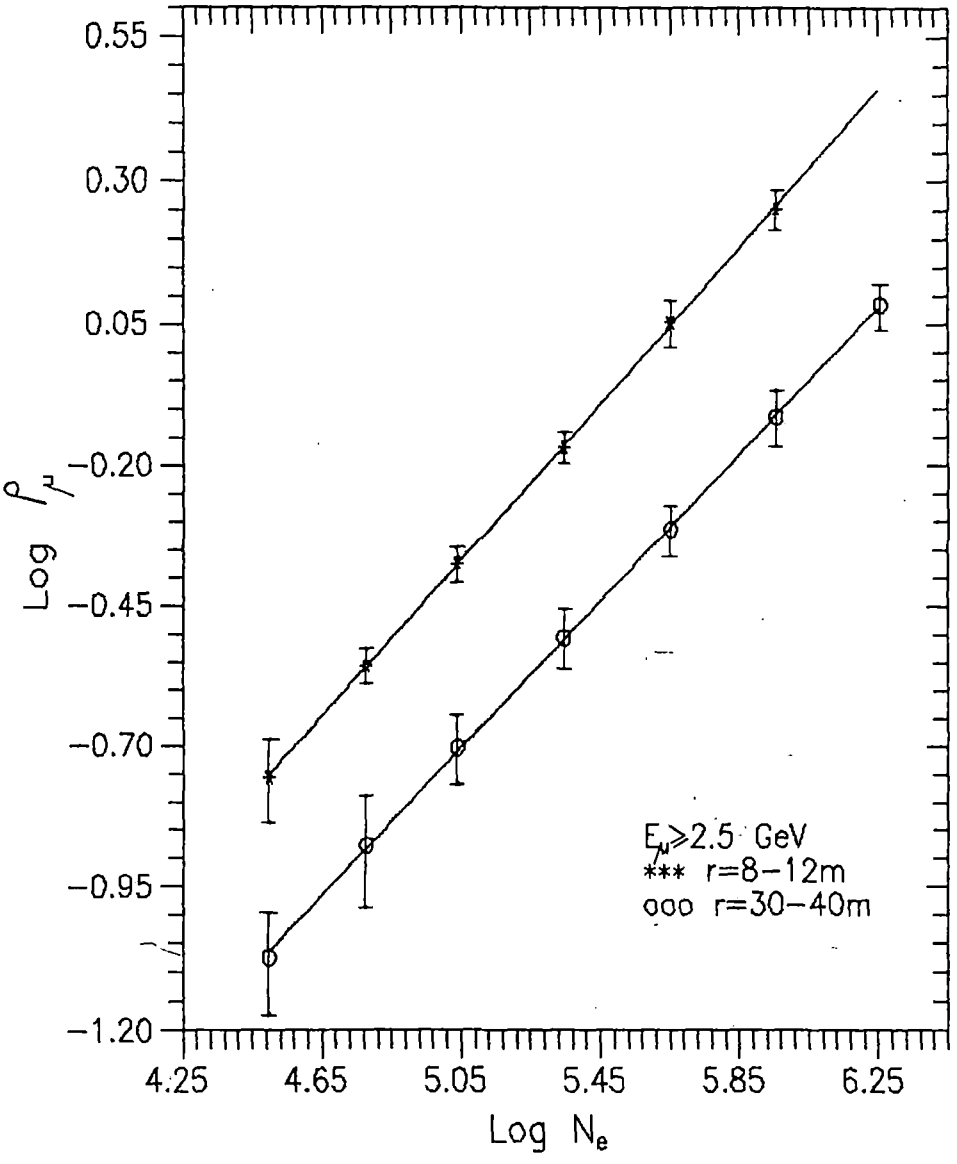

Fig.3.26. Variation of muon density at radial distance ranges 8−12m and 30−40m with shower size at muon threshold energy 2.5 GeV

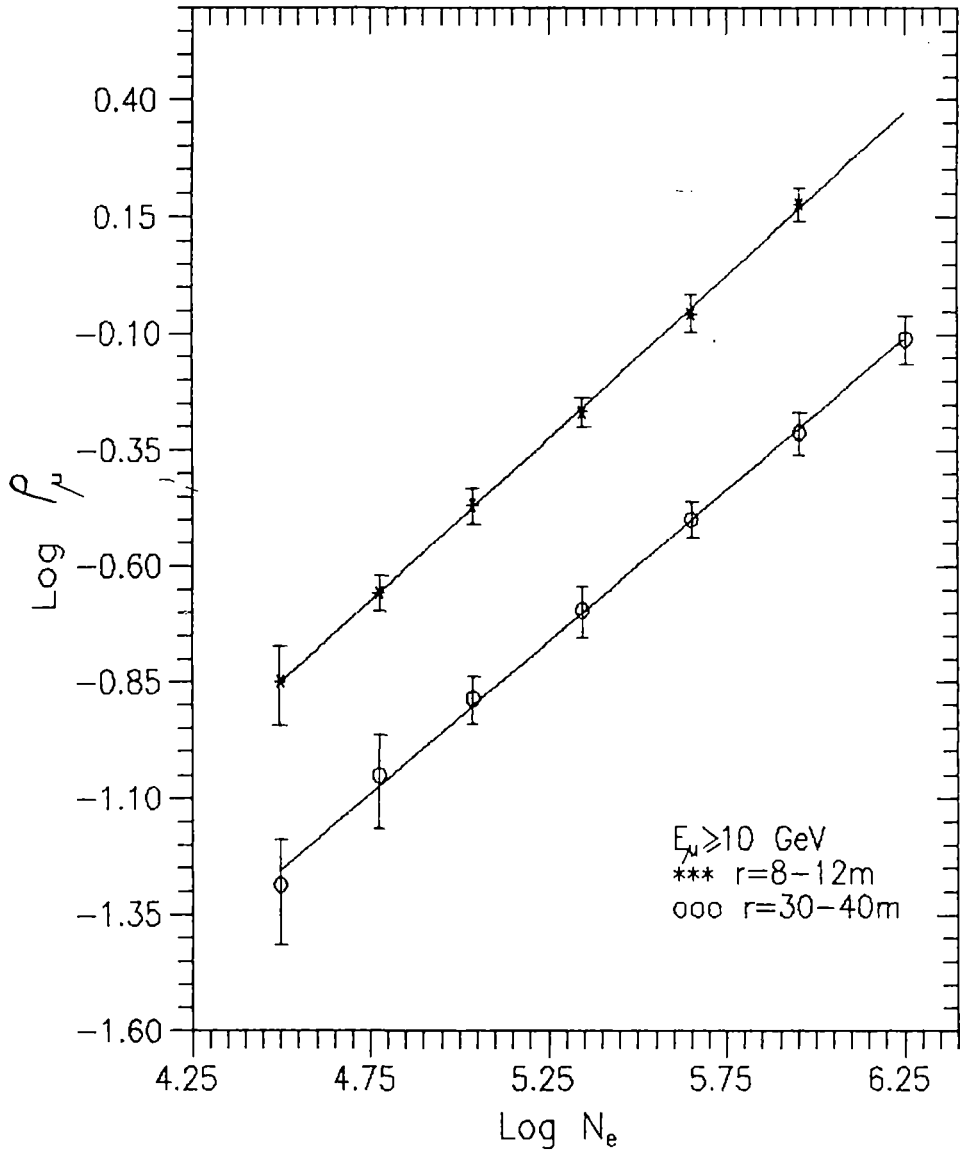

Fig.3.27. Variation of muon density at radial distance ranges 8−12m and 30−40m with shower size at muon threshold energy 10 GeV

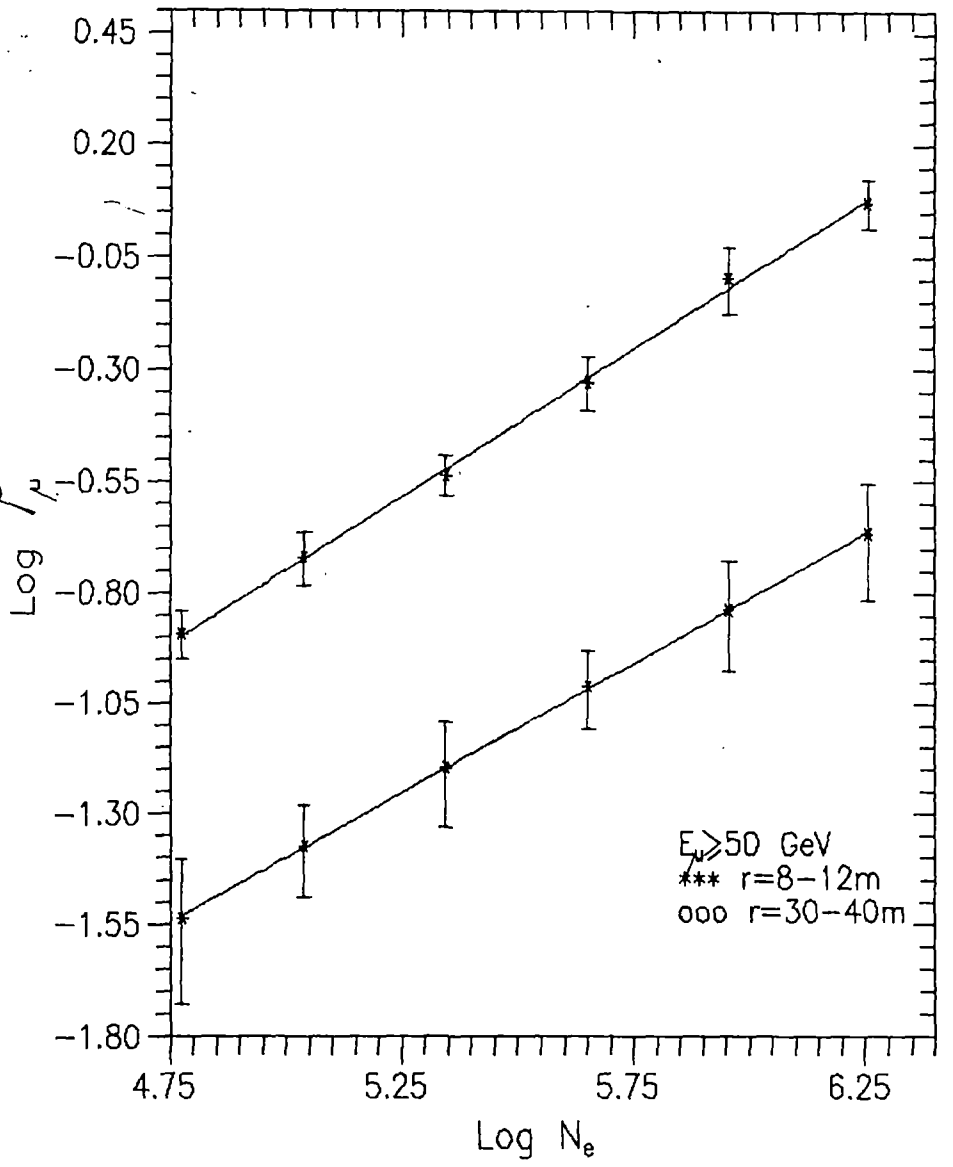

Fig.3.28. Variation of muon density at radial distance ranges 8−12m and 30−40m with shower size at muon threshold energy 50 GeV

A plot of this function for $N_e = 4.48 \times 10^5$ and $E_\mu \geq 2.5$ GeV is shown in fig.3.29 as an example .The value of α derived from this plot is 0.647. From fig.3.29 it is seen that except for the last radial bin ($\bar{r}$=34.1m) the shower cores were inside the edges of the array where the efficiency of the array is large. For the last radial bin , which is also close to the array boundary , obviously , the error of r and N_e are comparetively large but the overall effect of these errors on determination of α is small . The least square fitted line obtained from the plot of log ρ_μ vs. log r at various N_e for a particular muon threshold energy gives the values of α .

Values of α from the fit of the data for $E_\mu \geq 2.5$ GeV and $E_\mu \geq 10$ GeV are shown as a function of N_e in fig.3.30 and 3.31. The trend of α vs. N_e curves show that α is a function of N_e for N_e in the range 5.97×10^4 particles (primary energy 4.3×10^{14} eV) - 9.02×10^5 particles (primary energy 4.6×10^{15} eV) and becomes constant at higher shower sizes . For a lighter composition of the Primary Cosmic Rays it is expected to have steeper showers and hence large values of α.Therefore such a variation of α with N_e possibly indicates that the effective primary mass is decreasing from 4.3×10^{14}eV to around 4.6×10^{15}eV.

Y.Kawamura et al [17] and M.Ichimura et al [18] have derived similar conclusions about the primary mass in the knee energy region from direct observations from their new emulsion chamber experiments . From an analysis of low energy EAS muons Blake et al [19] reported similar trend for average primary mass in the primary energy region 6.0×10^{14} - 5×10^{15} eV.

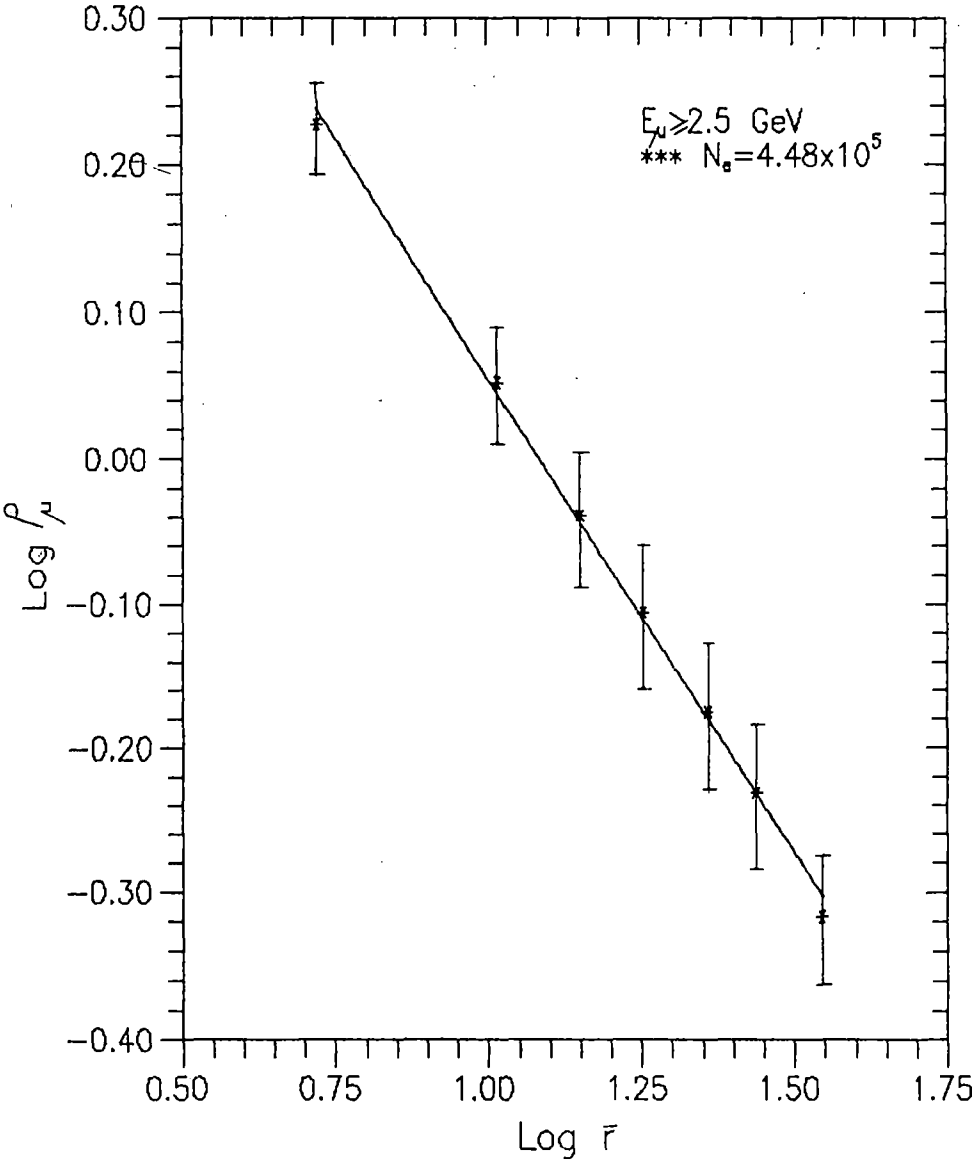

Fig.3.29. Variation of muon density with radial distance range for $N_e = 4.48 \times 10^5$

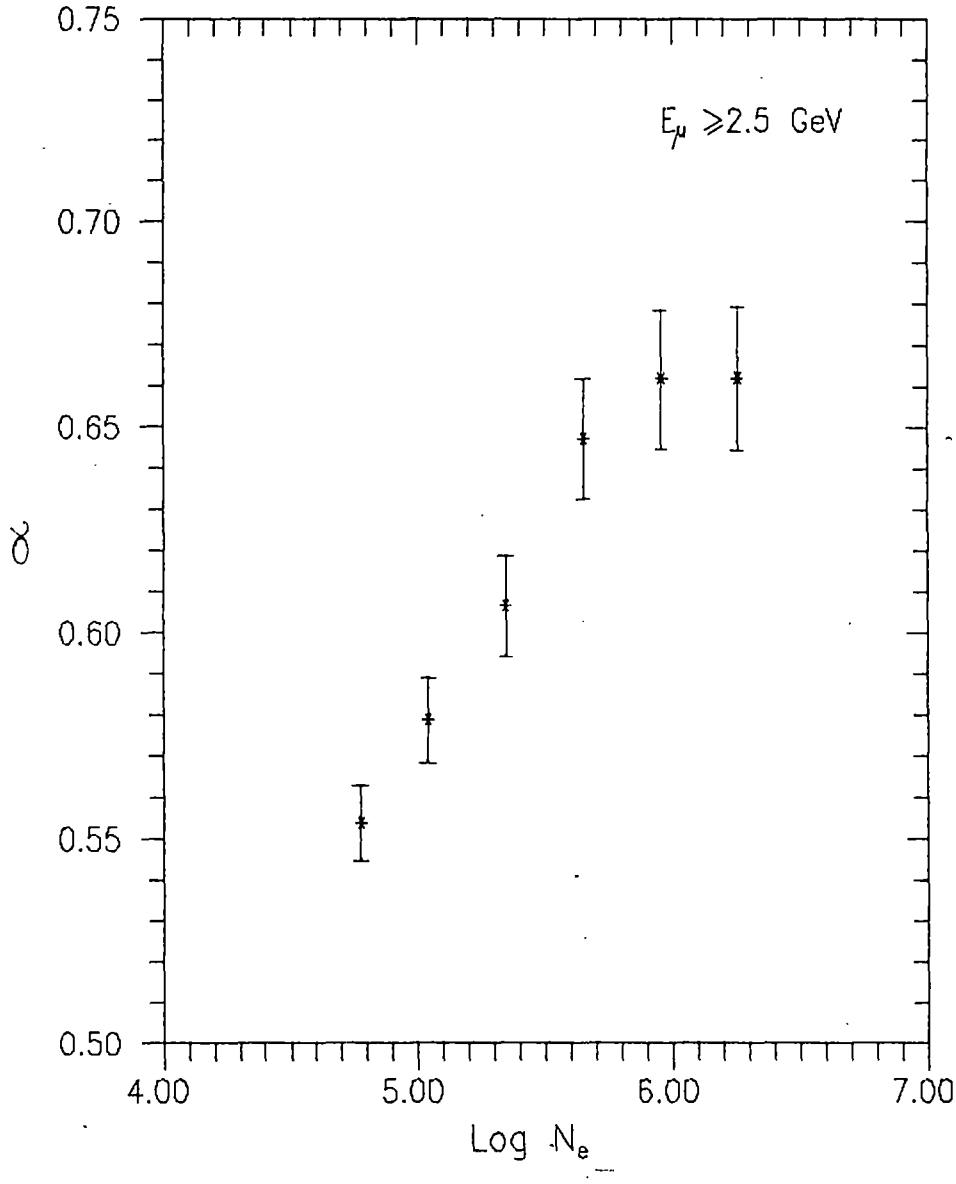

Fig.3.30. Variation of α with shower size (N_e) at the muon threshold energy 2.5 GeV.

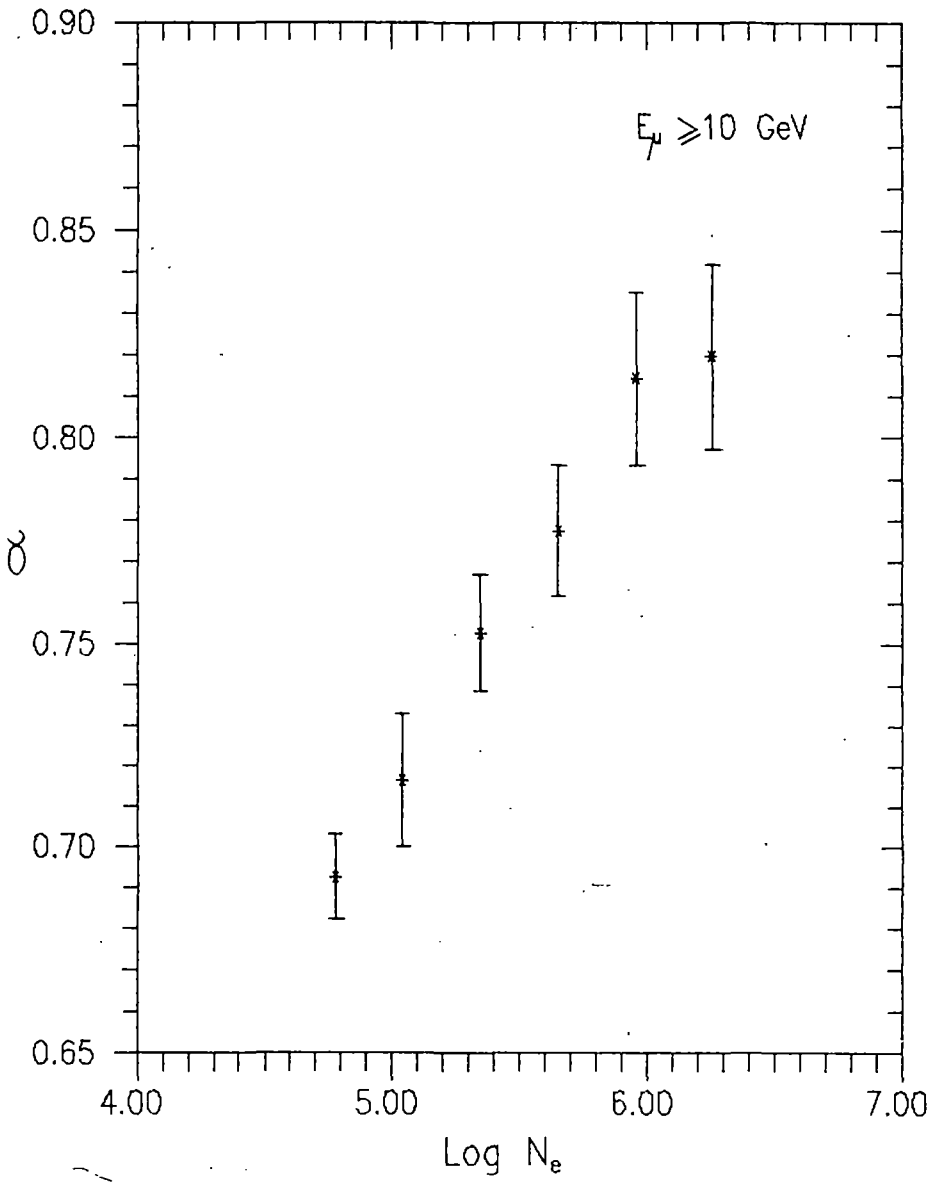

Fig.3.31. Variation of α with shower size (N_e) at the muon threshold energy 10 GeV.